

**Final Report to Government of Canada:
Climate Change Impacts and Adaptation Program,
May 2006**

**PROJECT A636:
LARGE SCALE MODELLING OF CANADA'S FOREST
ECOSYSTEM RESPONSES TO CLIMATE CHANGE**

Second Edition: 1 June 2006

David T. Price¹ and Daniel Scott²

Collaborators:

**Ronald P Neilson³, Ian Woodward⁴, Daniel W McKenney⁵, Dominique Bachelet⁶,
Jim Lenihan³, Mark Lomas⁴, Jon Foley⁷**

¹ Canadian Forest Service (CFS), Northern Forestry Centre, 5320-122 Street, Edmonton, AB T6H 3S5. Tel: (780) 435-7249; Fax: (780) 435-7359; E-mail: dprice@nrcan.gc.ca

² Faculty of Environmental Studies, University of Waterloo, Waterloo, ON, N2L 3G1, Tel: 519-888-4567 x5497, Email: dj2scott@fes.uwaterloo.ca

³ USDA Forest Service, Pacific Northwest Research Station and Department of Botany and Plant Pathology, Department of Forest Science, Oregon State University, USA.

⁴ Department of Plant and Animal Sciences, University of Sheffield, Sheffield, UK

⁵ CFS, Great Lakes Forestry Centre, Sault Ste. Marie, Ontario

⁶ Department of Biological and Ecological Engineering, Oregon State University, USA.

⁷ Institute for Environmental Studies, University of Wisconsin-Madison, Wisconsin, USA

Executive Summary

Simulating the effects of a changing climate on North American forests

The VINCERA (“Vulnerability and *I*mpacts of North American Forests to Climate Change: *E*cosystem *R*esponses and *A*daptation”) project involved vegetation modelling groups from Canada, the UK and the USA, each using a different Dynamic Global Vegetation Model (DGVM). The three DGVMs and their respective team leads were: IBIS - David Price of CFS, Northern Forestry Centre in Edmonton; SDGVM - Ian Woodward at University of Sheffield; and MC1 - Ron Neilson at Oregon State University. Each team ran their respective DGVM with a consistent data set for historical climate and six climate change scenarios that were developed by CFS (Price and McKenney). The suite of six climate change scenarios used three different Global Climate Models (CGCM2, HadCM3, CSIRO Mk2) and two Inter-governmental Panel on Climate Change (IPCC) emission scenarios (SRES A2 and B2) in order to reflect uncertainty in future climate conditions. The combinations of DGVMs and climate change scenarios were used to investigate the sensitivity of North American forest ecosystems to projected changes in climate, through key ecosystem parameters that included: Net Primary Productivity (NPP), Net Biome Productivity (NBP), total vegetation biomass and soil carbon, dominant vegetation type, and area burned.

In attempts to include IBIS, Price’s group encountered several problems which prevented them from obtaining acceptable results for present-day conditions. It was therefore unreasonable to use IBIS to project future responses. We continue to work to resolve these problems and we hope to have a complete set of IBIS results for North America available in the near future. Recent development work on IBIS is documented in Appendix I. In the mean time this report focuses on results obtained from the SDGVM and MC1 models, though some earlier results obtained from IBIS for southern Canada are presented for comparison.

Major findings

Applied to North America, the two dynamic vegetation models, MC1 and SDGVM, were remarkably similar in their simulation of year-to-year variations in 20th century productivity including net primary production (NPP) and NBP (= NPP minus losses due to disturbances and decomposition of dead material). Closer inspection showed that although these variations were strongly correlated, the NBP (i.e., net ecosystem carbon exchange) simulated by SDGVM was significantly higher (and generally positive) with most of this additional uptake accumulating in the soil C pools. On the other hand, MC1 maintained average NBP much closer to zero, with more carbon accumulating in vegetation biomass (such that simulated total ecosystem carbon densities were rather similar between the two models).

For the 21st century, the two models diverged greatly in their responses to the suite of forcing climate scenarios, with SDGVM simulating a strong positive effect of increasing CO₂ concentration on NPP, such that NBP remained positive and total

biomass and soil carbon continue to increase. Hence, according to SDGVM, North America's forests would remain as a net carbon sink throughout the 21st century. Conversely, MC1 generally shows an initial increase in NBP (albeit somewhat slower than SDGVM, because of lower sensitivity of NPP to increasing CO₂ concentration), followed by a serious decline from about 2030 onwards—due to increasing occurrence of droughts and, to a limited extent, increased areas lost to wildfire. By 2100 these projected differences in NBP lead, on the one hand, to significant gains in biomass carbon and total ecosystem carbon when simulated by SDGVM, but to significant losses when simulated by MC1 (with the CGCM2-A2 climate scenario causing the biggest declines). Neilson has described these as the “green-up” and “green-up followed by brown-down” projections, respectively.

The divergence between the two DGVMs far outweighed any differences in the responses of each model to the range of climate forcings produced by each of three GCMs and the two IPCC SRES emissions scenarios used to drive them. At the least, this finding indicates that ecosystem responses to climatic change are much less certain than the uncertainty implicit in the GCM climate scenarios. More broadly, this result demonstrates that the DGVMs are not yet reliable and require more development and testing. The differences between the two DGVMs (i.e., in their respective responses to the entire set of climate scenarios) appear to be caused primarily by the way in which they respond to the interacting effects of increased drought and increasing atmospheric CO₂ concentration.

The MC1 projections show the greatest carbon losses occurring in three major forested regions of North America, broadly grouped by Neilson et al. (2006), as western USA, eastern USA and the boreal (covering Alaska and much of western and central Canada). It is worth noting that a significant decline in forested cover and total carbon was also projected in earlier IBIS simulations for the western Canadian boreal region forced by the CGCM2 IS92A scenario (which closely resembles the CGCM2 SRES A2 used in VINCERA). More detailed discussion of regional changes in the ecosystem indicators identified above, as modeled by the different DGVM and climate change scenario combinations, is presented in Section 4 of the report. Numerous maps are presented, comparing results for each model in the year 2000 with those for each of the six climate scenarios in 2100.

At this stage it is difficult to determine which of the two sets of model projections is more believable. Recent review of CO₂ responses of stands at FACE (“Free-Air CO₂ Enrichment”) sites by Norby et al. (2005), suggests there is a generally positive response of tree-level NPP to increasing CO₂ concentration, but with the caveat that FACE rings are generally located in immature stands. On the other hand, Körner et al. (2005) provide strong evidence that mature stands (i.e., at or close to site carrying capacity) do not exhibit a sustained positive response to elevated CO₂. Interestingly, SDGVM shows a positive NPP response very consistent with the Norby et al. observations, due to its use of the well-accepted Farquhar leaf photosynthesis algorithm. Conversely, MC1 uses a much simpler empirical formulation for photosynthesis, and exhibits a much weaker NPP response. A second important difference is that MC1 has a relatively sophisticated fire model which responds to interannual climate variations and to spatial differences in fuel

densities, whereas SDGVM has a very simplistic fire model that removes biomass with very little dependence on fuel densities or sensitivity to climate. However, SDGVM burns on average about three times the area annually compared to MC1. Moreover, although SDGVM productivity is generally higher, biomass densities are maintained lower. This suggests that high fire in SDGVM may keep biomass density below observed carrying capacities and hence causes consistently positive productivity responses. A third, possibly important factor relates to how simulated vegetation responds to drought years: water use efficiency (WUE) is known to increase with increasing CO₂ concentration, but it differs greatly between the two models, evidently causing vegetation to die back much more in MC1 than in SDGVM. This mortality then feeds into litter production and fuel build-up, and may help to trigger more simulated fires in MC1.

The collaboration between the three DGVM teams and other partners initiated by the VINCERA project will continue as the teams work to better understand the different results produced by the DGVMs. As refined projections become available they will provide indicators of the “relative health” of Canada’s forests over periods of a few years to several decades. Interpreting model results in this way will provide a fundamentally new assessment of the impacts of climate change for forestry, protected areas and other forest users (i.e., to inform decision makers where and when significant changes in Canada’s forests are most likely, and how rapidly they may occur). This continued work will culminate in forthcoming publications that will be forwarded to the Climate Change Impacts and Adaptation Program as they become available.

Future work – resolving the disagreement

More work is clearly required to determine the true nature of the response of NPP to rising CO₂ concentration for a range of forested ecosystems. I.e., is the positive response presently seen at FACE experiments likely to be maintained as stands reach maturity? Other questions requiring attention include:

1. What are the critical relationships among climate, vegetation productivity and area burned in temperate and boreal forests of North America, and can this be adequately captured in dynamic vegetation models?

What are the likely impacts of soil water deficits, as a function of soil hydrology, and CO₂ concentration effects on WUE, on forest vegetation under plausible scenarios of future climate?

1 Introduction

The forests and other natural ecosystems covering continental North America are being subjected to significant environmental stresses resulting from a combination of human activities. Global change includes damage to and loss of natural ecosystems due to exploitation, mismanagement and land use conversion, and the effects of numerous pollutants on land, and in air and water. However, one of the most pervasive anthropogenic pressures results from increasing atmospheric concentrations of greenhouse gases (GHG), due mainly to consumption of fossil fuels and tropical deforestation. There is now little doubt that this accelerating increase in GHG concentration has already caused detectable changes in global climate and is likely to cause greater changes in the coming decades (IPCC 2001). Climate change threatens global ecosystems both in structure (distribution, size and species composition) and in function (growth, mortality, regeneration and decomposition). A series of meta-analyses (Hughes 2000, McCarty 2001, Parmesan and Yohe 2003, Root *et al.* 2003) have compiled evidence that biological systems are already responding to the changing climate of the twentieth century.

Forests are of critical importance in the natural heritages of the USA and Canada, as well as to their respective economies. They support tourism and recreation, and ecosystem diversity, as well as providing timber, habitat for wildlife, and many other products. In their natural state, North American forests contribute vital ecosystem functions including, stabilization of the global climate, cycling of fresh water and the sequestration of carbon. Climate change threatens all of these forest services, as well as the social and economic infrastructures they support, but the magnitude of this threat is unclear and difficult to estimate.

The primary problem in quantifying the effects of a changing climate on any natural ecosystem is *uncertainty*. Because the future is unknown, and because the effects of gradual changes on the slow processes inherent in many forest ecosystems are themselves difficult to detect; we are dependent on process modelling as a method of investigating the sensitivity of ecosystems to a range of uncertain futures. But more than this, the models available both to predict the future climate, and to simulate the possible large-scale responses of ecosystems to climatic changes, are by necessity highly simplified representations of reality that compound these uncertainties.

Earlier modelling studies of vegetation distribution in Canada were based on results obtained using *equilibrium projection* biogeography models (e.g., Rizzo and Wiken 1992; Lenihan and Neilson 1995; Neilson 1998). These studies all projected some very significant changes in the distribution of boreal and temperate forests, but their value was limited because the simulated vegetation distribution relies on correlations established between the present-day observed vegetation distribution and climate. Hence, the future projections implicitly assume that all vegetation zones are fully adapted to future climate (i.e., vegetation structure and function are in a quasi-stable state, and determined by a “stabilized” global climate). Aside from the question of whether a stabilized climate can occur in the foreseeable future given recent perturbations (i.e., next 200-500 years), it is likely that it would take centuries, if not millennia, for all vegetation

biomes to become fully equilibrated to that stabilized climate (e.g., Overpeck et al. 1992). This would likely be particularly true in high latitude regions where shallow soils and cold climates presently limit soil water and nutrient supplies and hence constrain vegetation productivity and the build-up of soil carbon pools (e.g., Price et al. 1999). Hence a major limitation of equilibrium models is that they are unsuited to projecting possible responses of natural and extensively managed ecosystems over the next 50-100 years, i.e., over a period consistent with long-term planning horizons, as required in forest or protected area management plans and community adaptation programs.

The VINCERA (“Vulnerability and Impacts of North American Forests to Climate Change: Ecosystem Responses and Adaptation”) project reported here was designed to overcome these limitations by comparing the results of *dynamic* ecosystem models used to simulate changes in vegetation distribution and biogeochemical cycling under climate change. Dynamic Global Vegetation Models (DGVM) (e.g., Foley et al. 1996; Beerling et al. 1997; Daly et al. 2000; Cramer et al. 2001; Bachelet et al. 2003) have the potential to overcome many of the limitations in equilibrium projection simulations. These models can project short-term (decadal) transient responses to climate change, making no assumptions about the long-term correlation of vegetation distribution to climate. Vegetation is simulated *dynamically* as combinations of Plant Functional Types (PFT), which respond to environmental conditions that can change continuously, including climate, atmospheric CO₂ concentration, natural disturbances and even human actions. Dynamic vegetation processes that are typically represented include: photosynthesis and respiration; competition for light, water and nutrients; natural disturbances such as fire; plant phenology; and soil decomposition; though the algorithms adopted to represent them may vary significantly between specific models.

This model inter-comparison study used the results of three different DGVMs operated by research groups from the UK and the USA as well as Canada. In many ways, VINCERA was intended to be a continental scale extension of the well-known Vegetation/ Ecosystem Modeling and Analysis Project (VEMAP, VEMAP Members 1995; <http://www.cgd.ucar.edu/vemap/>) carried out by a large group of researchers in the late 1990s, but focused on the ecosystems in the conterminous USA. As with VEMAP, the objectives were to investigate possible impacts of climate change and increasing atmospheric CO₂ concentration on the key attributes of forests and other natural ecosystems. Three different DGVMs were compared, each driven by the same suite of six scenarios of future climate taken from the projections simulated by three state-of-the-art global climate models. A continental soils dataset was also constructed from available data to ensure as much consistency as possible in the forcing data sets.

2 Objectives

The overall objectives of VINCERA were to assess:

1. the impacts of a range of plausible climate change scenarios on the distribution, productivity and composition of Canada’s forests, and
2. the implications of these impacts for forestry and conservation interests.

A third objective originally proposed was to carry out simple risk assessments for major geographic regions within the North American continent, based on the “most likely” scenario results and following discussions among stakeholders and the research team. As will be made clear, fundamental limitations with all three DGVMs, in their current state of development, prevented us from addressing this third objective.

3 Methods

3.1 Climate scenarios

The earlier studies of projected vegetation changes in Canada reported above were based on equilibrium ($2\times\text{CO}_2$) climate projections obtained from earlier (uncoupled) General Circulation Models (GCM) forced with the IPCC’s IS92a emission scenario. The current state of the art approach is to use the results of fully coupled, transient GCMs (such as the Canadian CGCM3 or UK Hadley Centre HadCM3) forced with the latest IPCC emission scenarios (SRES series). In the lead-up to its 2001 Third Assessment, the Intergovernmental Panel on Climate Change (IPCC) also formulated a suite of GHG emission scenarios based on different projections of human demographics and global and regional economic growth, captured in the IPCC Special Report on Emissions Scenarios (SRES; <http://www.grida.no/climate/ipcc/emission/>). As the sophistication of GCMs has grown, so has the number of models providing projections of climate changes under the range of SRES scenarios (<http://ipcc-ddc.cru.uea.ac.uk/>). This combination of many GCMs and multiple emissions scenarios gives rise to a potentially very large numbers of climate projections, each of which is likely to have different magnitudes of changes, for different climate variables, occurring over different regions and different time-frames.

High resolution climate scenarios were developed by the Canadian Forest Service’s (CFS) Great Lakes Forestry Centre in collaboration with the Northern Forestry Centre (see McKenney et al. 2006b; Price et al. 2004). CFS had previously developed a method for interpolating GCM output to 5 minute (1/12 degree) resolution (Price et al. 2001) using the ANUSPLIN spline-fitting interpolation method developed by Hutchinson and coworkers (e.g., Hutchinson 1998, 2004; Hutchinson and Gessler 1994; see also Price et al. 2000). The method requires the creation of a baseline of observed climate, in this case high resolution interpolation of 1961-90 climate normals from several thousand weather stations across Canada and the USA (see McKenney et al. 2004, 2006a). This interpolation was “tri-variate”, i.e., it took elevation effects on each climate variable into account as well as latitude and longitude. The interpolated estimates therefore have greater spatial variation than would be obtained by considering latitude and longitude alone. Tri-variate ANUSPLIN “surfaces” were developed for each of six key monthly climate variables: mean daily maximum and minimum temperatures, precipitation, downward incident total solar radiation, wind velocity and vapour pressure.

Climate simulation results covering North America were obtained for three different GCMs using each of the SRES A2 and B2 greenhouse gas (GHG) emission scenarios. Simulation results from the Canadian Global Climate Model (CGCM2) were obtained from the Canadian Climate Centre for Modelling and Analysis (CCCma <http://www.cccma.bc.ec.gc.ca>), while those from the UK Hadley Centre (<http://www.metoffice>

[.com/research/hadleycentre/index.html](http://www.csiro.au)) GCM (HadCM3) were obtained from the IPCC Data Distribution Centre (IPCC DDC, <http://ipcc-ddc.cru.uea.ac.uk/>). The third model was the Australian CSIRO Mk2 developed by the CSIRO Atmospheric Research Laboratory (<http://www.csiro.au>). In this case some files were obtained from IPCC DDC but specific humidity data were obtained directly from CSIRO on personal request. Time series of historical and projected changes in atmospheric CO₂ used in the IPCC A2 and B2 emissions scenarios were obtained from Ron Stouffer at GFDL, Princeton, NJ.

Processing the GCM output data followed the approach used for VEMAP (VEMAP Members 1995) and is described in greater detail in Price et al. (2004), so only a brief description will be provided here. For each simulated climate variable, the means of each monthly value over the period 1961-90 were first calculated at each GCM grid node¹. These means were then used to convert the raw GCM data into monthly “pseudo-anomalies”, either by subtracting the computed 1961-90 means (in the case of temperature data) or by dividing by them (in the case of all other climate variables). The pseudo-anomalies were then interpolated using ANUSPLIN to create monthly bi-variate surfaces (i.e., using only latitude and longitude as independent variables) at the same 5 minute resolution grid used for the 1961-90 climate normals. The interpolated GCM pseudo-anomalies for each climate variable were combined with the corresponding interpolated climate normals (added in the case of temperature, multiplied in the cases of other variables) to produce a set of monthly time series of projected values.

It should be understood that the primary objective in creating these climate scenarios was to combine the richness of observed climatological data (which reflect the critical influence of land surface topography on spatial variability), with the long-term trends in means and interannual variability projected by the GCMs, as forced by each GHG emissions scenario.

Climate scenarios were then constructed for input to the DGVMs, by joining available twentieth century time series of monthly data with the climate scenarios for the period 2001 to 2100 (or 2099 in the case of the Hadley Centre GCM). For temperature and precipitation, the historical data were interpolated from climate station observations in Canada and the USA for 1901-2000 using ANUSPLIN by McKenney et al. (2006a). Original climate station records were obtained from Meteorological Service of Canada (<http://www.msc-smc.ec.gc.ca>) and from the US Weather Service (<http://www.nws.noaa.gov>). In the case of vapour pressure and cloud cover fractions, historical data for this period were extracted from the UK Climate Research Unit (CRU) CRU TS 2.0 0.5 degree resolution global data set (Mitchell et al. 2003, submitted). Historical wind velocity data were not needed and not prepared. In addition, detrended time series were created from each of the five historical time series. The data were smoothed using a 30-year moving window average, and the smoothed values subtracted from (temperature variables) or divided by (other variables) the original data to create a time series of detrended anomalies. In addition, mean values were calculated for each month at each grid node over the period 1901-1915. This period was used as the baseline for detrending (rather

¹ Use of the term “grid node” here is intended simply to indicate that GCM output data are strictly applicable to the corners of gridcells, whereas the interpolated data are considered to apply to the centroids of the higher resolution gridcell used to report DGVM output.

than the entire 1901-2000 period) because decadal scale variations in some variables, notably minimum temperature, persisted in the detrended anomalies. Using 1901-1915 as the baseline removed any tendency for a step change between the end of the detrended data and the start of the twentieth century time series. It was found that such step changes could destabilize previously “equilibrated” carbon pools. The detrended anomalies were then combined with the monthly means (i.e., added for temperature, multiplied for other variables) to create the final detrended time series. These data were used for model initialization before beginning the simulations for the period 1901-2100.

3.2 Soils Data

A soils data set covering North America did not exist previously and needed to be compiled from available sources: the Canadian Soils Information System (CanSIS) Soil Landscapes of Canada (SLC) Version 2.2 database, the US VEMAP soils data set and the Alaskan State Soil Geographic (STATSGO) data set. This data set provides soil texture information for depths down to 1.5 metres, split into three layers at 0.5 degree resolution covering North America. Additionally, the dominant soil types (or “components”) are represented within each 0.5 degree gridcell by area fraction, with up to four mineral and one organic component reported. These data are also able to be used for a higher resolution data set (10 km) covering Canada and Alaska, although this work has yet to be completed.

A key feature of this dataset, as compared to some earlier global data sets, is that the texture data are generalized according to the dominant soil types rather than being simple averages of reported sand, silt and clay fractions. The problem with averaging is that gridcells having mixtures of relatively discrete regions of clay soils and pure sandy soils become “loams” when averaged, with altogether different effects on vegetation productivity. Having compiled these dominant soil types, a subset of the data was distributed to the US and UK groups (who only required one soil type per gridcell). This consisted of the largest area component being assumed to cover each gridcell, and thus avoided the averaging problem while keeping the number of gridcells manageable.

A more detailed technical description of the VINCERA soils data set is presented in Appendix II.

3.3 Dynamic Vegetation Model simulations

Even though the representation of many vegetation processes is necessarily relatively simplistic in DGVMs, these models are highly complex and have high computational requirements (particularly at high resolution). The outputs of these models are important diagnostic ecosystem variables, including evapotranspiration and runoff, vegetation composition, and carbon balance indicators such as Net Primary Productivity (NPP) and Net Biome Productivity (NBP).

The VINCERA project brought together DGVM research groups from Canada, the UK and the USA. A suite of six scenarios of 21st century climate, derived from different GCMs by Canadian Forest Service (CFS) researchers (McKenney et al. 2006b; Price et al. 2004), was used to investigate sensitivity of North American forest

ecosystems to projected changes in climate, modelled at 0.5 degree gridcell resolution. Each DGVM team (led by David Price at CFS Northern Forestry Centre in Edmonton, Ian Woodward at University of Sheffield, and Ron Neilson at Oregon State University), used a different DGVM driven by consistent historical climate data for 1901-2000 and six climate scenarios for 2001-2100. As indicated, both the historical data set and the climate change scenarios were developed by CFS staff and provided to the collaborating DGVM teams in the UK and USA.

The three DGVMs used in VINCERA were (a) MC1, developed by Ron Neilson and coworkers at Oregon State University; (b) SDGVM, developed by Ian Woodward and colleagues at Sheffield University in the UK; and (c) an extensively modified version of the IBIS model of Foley et al. (University of Wisconsin, Madison), being developed for application to Canada by Price and coworkers at CFS (e.g., El Maayar et al. 2001). It should be stated that Price's group has had numerous problems in trying to apply IBIS to Canada and the USA at a higher spatial resolution. Our work continues and although we have made a lot of progress, to date we have not been able to generate what we consider scientifically acceptable simulation of present-day forest distribution at the continental scale, with credible values for key ecosystem indicators, including NPP and NBP. Appendix I provides a summary of modifications that have been implemented in our Canadian development version of IBIS (referred to as "Can-IBIS").

Both MC1 and SDGVM combine representations of productivity and respiration including responses to atmospheric CO₂, soil water and nutrient limitations, with competition among plant functional types (PFT) and with simulation of the occurrence of wildfires. The MC1 model (e.g., Bachelet et al. 2005), combines elements of the MAPSS biogeography model with CENTURY biogeochemistry model and a relatively complex fire model, based on well-accepted algorithms from the wildfire modeling community in Canada and the USA. The CENTURY model of soil biogeochemical cycling has been well-validated for a range of ecosystems around the world, but has a relatively simple representation of aboveground processes—in particular an empirical canopy productivity model.

The SDGVM model includes a detailed model of canopy processes based on the Farquhar photosynthesis model, merged with CENTURY's algorithms for biogeochemical cycling, but a relatively simple fire model. Both SDGVM and MC1 simulate responses of a relatively small number of Plant Functional Types (PFTs) to climate in both an overstory and an understory, which compete with each other to result in a dynamic ecosystem over time. The resulting PFT mixtures can be classified into descriptive vegetation types, although this was not done with SDGVM in the study reported here.

4 Results

The project has produced some important results, though these are by no means definitive and work is still in progress to resolve some of the fundamental questions that have been raised. Because of the problems encountered with IBIS, the results reported here include a summary of earlier simulations applied to Canada with IBIS, as a background to the more recent results obtained from SDGVM and MC1 applied to North America. We plan to carry out a definitive set of comparable Can-IBIS simulations for North America in the very near future.

4.1 IBIS simulations of Canada's forest ecosystem responses to climate change

Earlier unpublished large-scale simulations using the original Foley et al. (1996) IBIS model were forced by climate normals data for 1961-1990 and projections of climate change derived from the Canadian CGCM2 transient coupled GCM forced in turn by the IPCC IS92A (greenhouse gases + aerosols) emissions scenario. The results suggested that a warmer climate, with little or no significant change in precipitation patterns, would have some major impacts on Canada's forests. Figures 1 and 2 show simulated distributions of NPP for 2000 and the changes in NPP between 2000 and 2070. It should be emphasized that the estimates of present-day NPP are not very realistic: the lowest values are too low, but in relative terms the spatial distribution appears reasonable. Summarizing these results, for the west coast, where the climate is already mild and wet, small increases in NPP would be limited to those resulting from higher CO₂ concentration (probably leading to little or no significant change in NBP). The central region, lying between the Rockies and Lake Winnipeg, but also including interior BC, is already subject to relatively low rainfall, particularly in Alberta and Saskatchewan, and therefore more prone to wide scale droughts. Here the IBIS results indicate that the main effects of a warmer climate would be to further reduce average productivity, due to increased drought.

Figures 3 and 4 show maps of simulated natural vegetation distribution for 2000 and 2070. It should be noted, of course, that these maps do not allow for conversions of natural ecosystems to agricultural and urban uses. Bearing this in mind, the map for 2000 appears as a fairly credible representation of present-day vegetation cover, with some caveats regarding the band of grassland reported between the temperate and boreal forests of Ontario and Québec. For 2070, the central region shows a significant decrease in forest cover, as the simulated forests succumb to increased evaporative demand and are replaced by grassland and shrubland similar to the present-day prairies. When combined with increased die-back, higher decomposition rates, and fires, the central region would likely undergo significant carbon losses, and hence negative NBP. In the east, (including much of Manitoba) where present-day productivity is limited primarily by temperature, NPP would be expected to increase due to the combined effects of longer growing seasons, greater nitrogen cycling and higher CO₂ concentration, leading to significant increases in NBP. There are some contradictions to this general story: note for example

the slight increases in NPP in southern Saskatchewan seen in Fig. 2, which are related to the simulated expansion of temperate deciduous forest into this region (Fig. 4).

The changes in NPP lead to some projected changes in vegetation biomass, shown in Figures 5 and 6. It should be noted that IBIS generally underestimates forest biomass, particularly in coastal regions where undisturbed forest stands can often achieve 250 tonne C ha⁻¹, compared to the maximum simulated densities of around 10 kg C m⁻² (or 100 tonne C ha⁻¹). This underestimation problem appears even worse for the prairie provinces which report little or no biomass at all, even where NPP is relatively high. Part of the explanation for this apparent contradiction is that much of the NPP in the central boreal forest region is attributed to understory vegetation (herbs and shrubs), which do not accumulate much biomass over a one year period. With these caveats in mind, however, the broad distribution of simulated biomass density across the country is somewhat consistent, in relative terms with observations. The simulated changes then show losses of biomass in the west and southern boreal with significant gains in much of the east, and to some extent in the boreal regions of northern Saskatchewan and Manitoba. There is also a band of major biomass decrease extending across Ontario and southern Québec over to Newfoundland. This is explained by the projected change in vegetation where trees give way to grassland and shrubs seen in Figure 4. However, the westward expansion of temperate deciduous forest suggests this decline is really a temporary state, where the boreal forest vegetation is about to be replaced by temperate deciduous forest.

A significant departure from this general rule occurs in a band crossing Ontario and southern Quebec. This is explained by a projected change in vegetation, where IBIS also suggested that in some regions, notably central and northern Alberta and to some extent the central interior of BC, there would be significant loss of forests to be replaced by ecosystems dominated by grasses and shrubs.

Some important caveats concerning these projections using IBIS are:

1. Historical climate data used for baseline (2000) ecosystem states were simply 1961-90 climate normals with no interannual variations.
2. Only a single climate scenario (CGCM2 model forced by IPCC IS92A emissions scenario), was used to examine the potential impacts of climate change.
3. Standard IBIS simulation assumes a uniform 4 m soil depth.
4. Constraints were imposed on NPP assuming static nitrogen limitations.
5. In spite of 4, simulated present-day NPP seems too low (in comparison to other models and to what we know from relatively few field measurements).

These caveats led to an extensive effort to try to resolve these and other limitations of the model, primarily to improve IBIS' simulation of NPP for boreal ecosystems (see Appendix I for a more detailed record of these efforts).

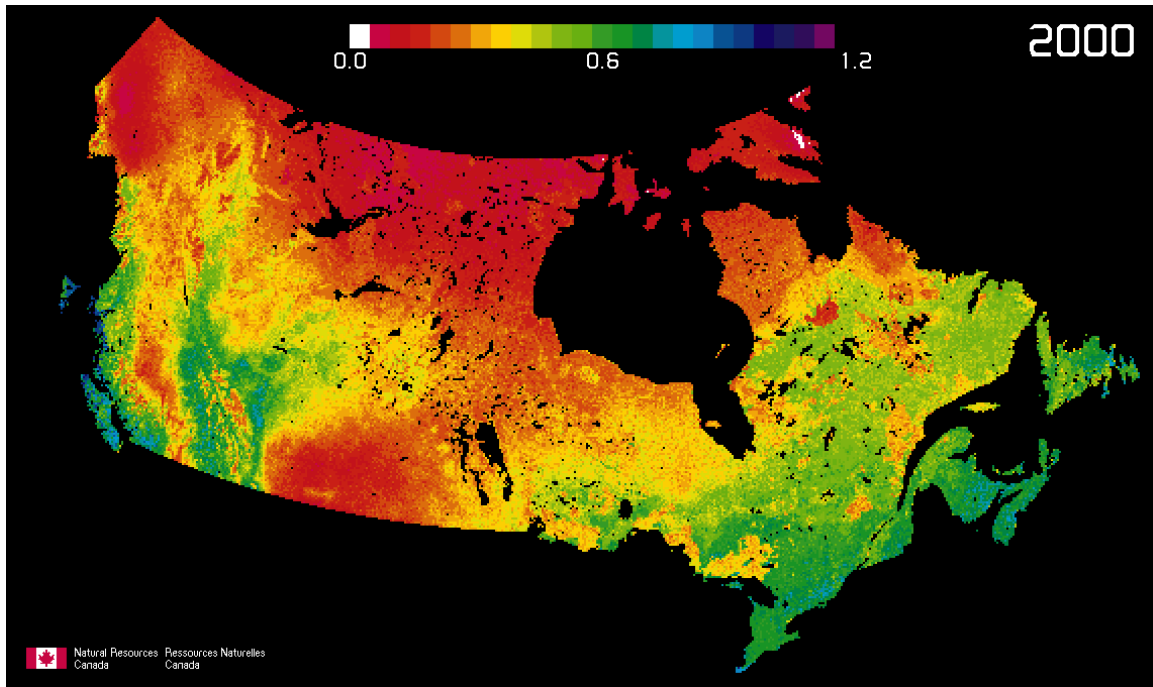


Figure 1. Net Primary Productivity (NPP, $\text{kg C m}^{-2} \text{ yr}^{-1}$) as simulated by IBIS for 2000. Note the unrealistically low values for much of the grassland and boreal forest regions in the Prairie Provinces and for all ecosystems in interior B.C.

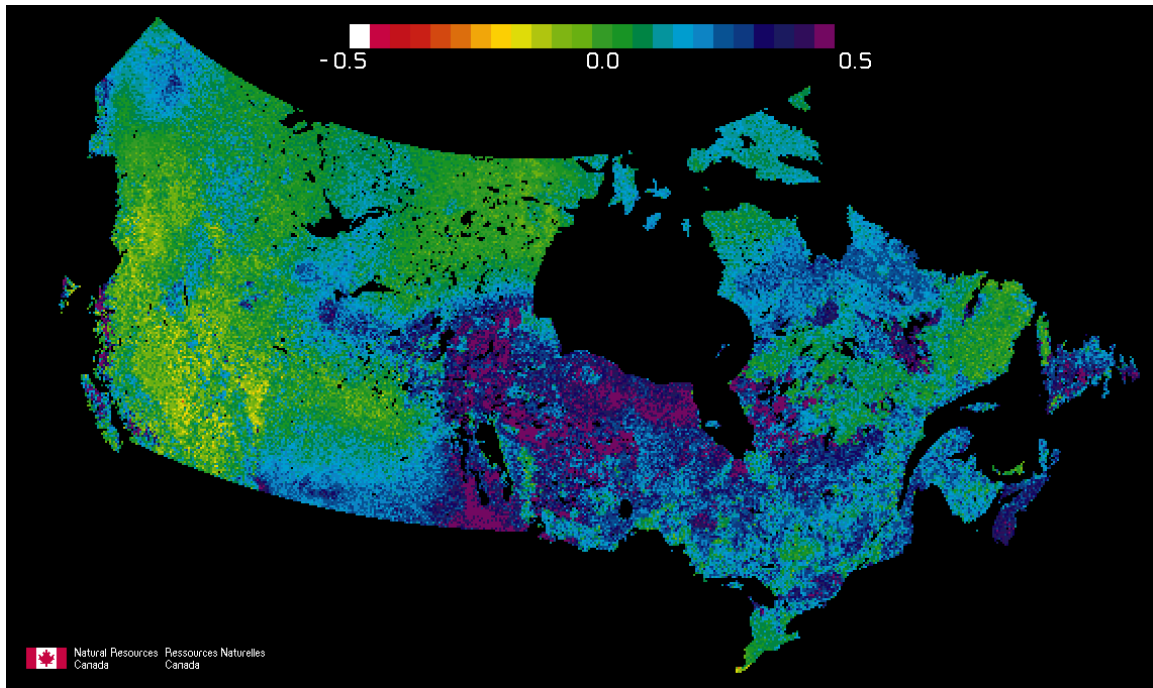


Figure 2. Changes in NPP ($\text{kg C m}^{-2} \text{ yr}^{-1}$) as simulated by IBIS for the period 2000 to 2070 (a positive value indicates an increase).

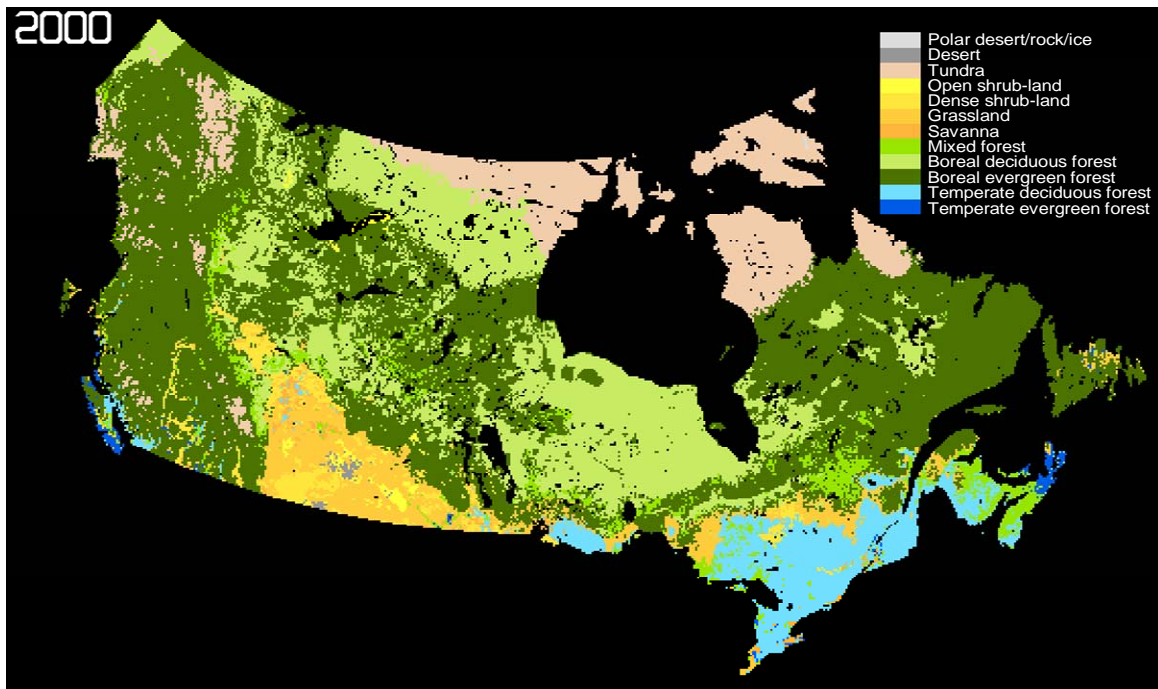


Figure 3. Distribution of major vegetation types as simulated by IBIS for 2000. Note the questionable band of grassland types extending across Ontario and southwestern Quebec and the incorrect simulation of temperate deciduous forest just west of Lake Superior.

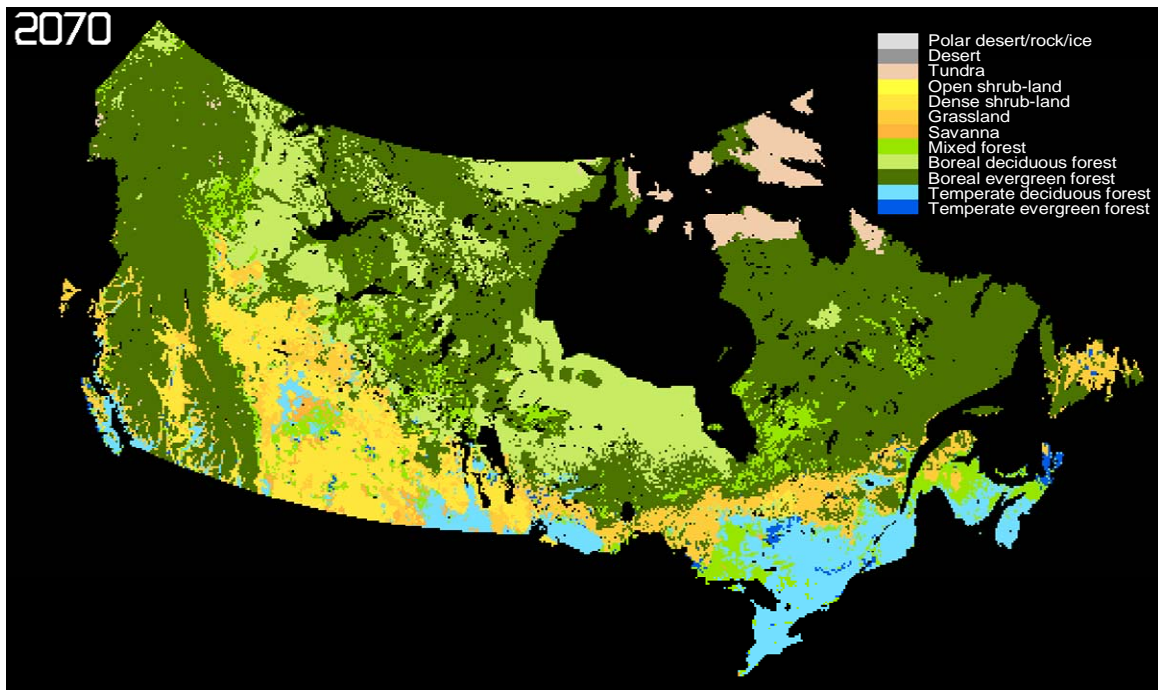


Figure 4. Distribution of major vegetation types as simulated by IBIS for 2070.

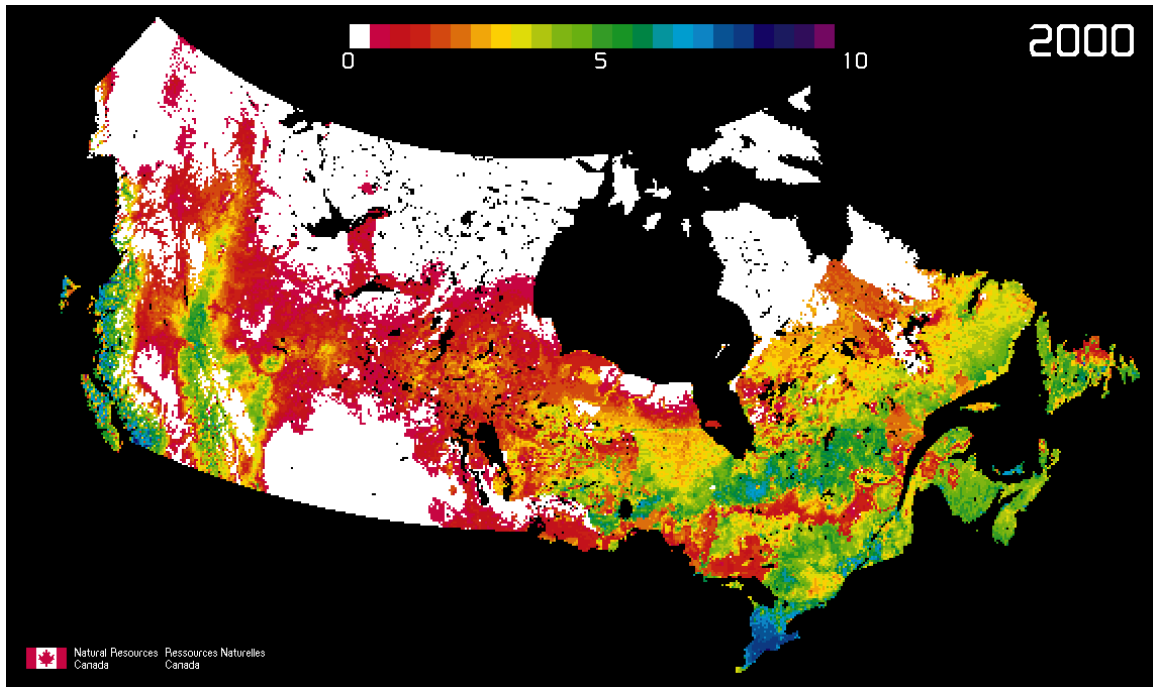


Figure 5. Forest biomass distribution (kg[C] m⁻²) as simulated by IBIS for 2000. Note the very low values estimated for the prairie Provinces, interior BC and the band across central Ontario and southern Québec.

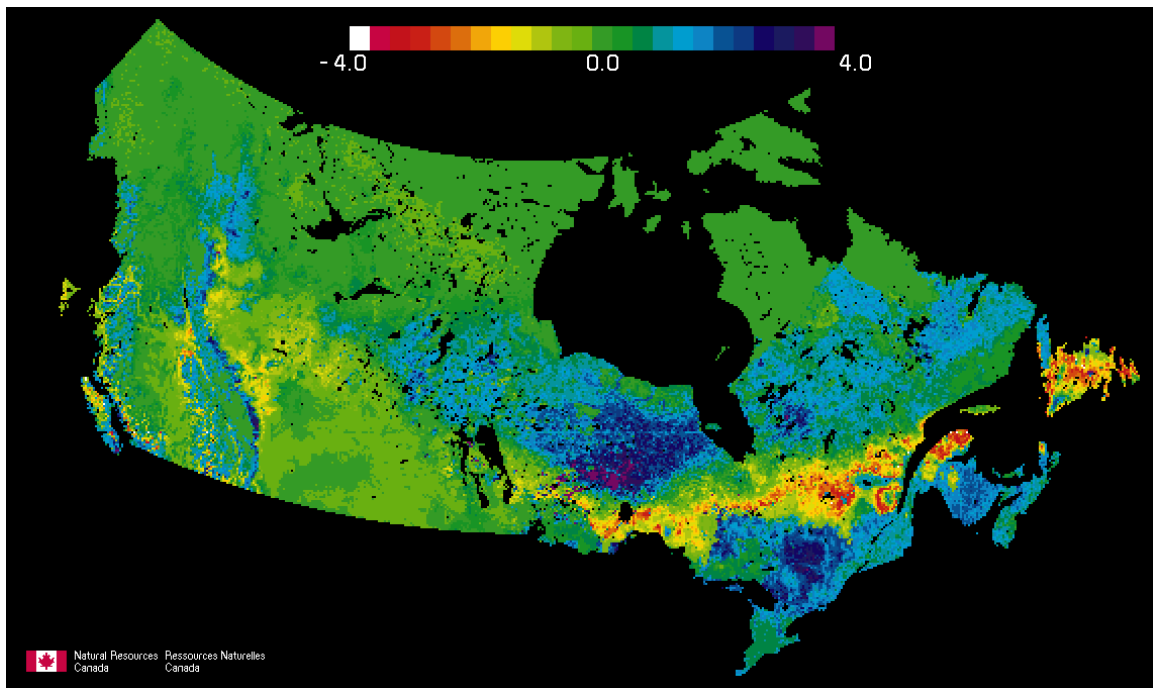


Figure 6. Changes in biomass (kg[C] m⁻²) as simulated by IBIS for the period 2000 to 2070 (positive value indicates increase). The obvious decreases seen in southern Manitoba and extending across Ontario and southern Québec into the Maritime provinces are evidently related to the replacement of forest by grassland and shrublands seen in Figs. 3 and 4.

4.2 **VINCERA results for North America**

The remaining discussion focuses on the VINCERA results obtained in 2005-06 by the SDGVM and MC1 teams.. Work is still in progress to resolve some of the fundamental questions that have been raised, with results to be the subject of a paper in preparation.

The most surprising initial result was that the future projections of North America's forests differed very significantly between SDGVM and MC1. As will be seen from all the graphs and maps presented in the following pages, *the differences between the models' simulations of vegetation responses were far greater than any differences that could be attributed to the different GCM climate scenarios*. Figures 7-10 show graphs of the continental scale area-weighted averages² of four key indicators simulated by both models: total biomass carbon and total soil carbon, and average NPP and NBP, each simulated both for the 20th century from available historical climate data and for each of the future GCM projections.

Comparison of the estimates of total biomass carbon and soil carbon storage in Canada and the USA during the 20th century shows significant differences between the two models, though interestingly the estimates of *total ecosystem carbon* (i.e., vegetation and soils) are rather similar (approximately 37 Pg C fro MC1, compared to 34 Pg C for SDGVM).

Simulated estimates of NPP also differ substantially for the 20th century, with MC1 initially higher but showing a much weaker increase over time. With the CO₂ concentration increases and climatic changes projected for the 21st century, SDGVM overtakes MC1, around 2040. Consequently biomass and soil carbon pools both increase consistently according to SDGVM. MC1's projections for the future are very different: total biomass increases slightly for 30-50 years (depending on climate scenario), but then goes into serious decline around 2030-2050 (the magnitude and timing vary among the climate scenarios, see Figure 7), while soil carbon is projected to decrease gradually starting as early as 2000 (Figure 8). Figure 10 shows that the modelled estimates of NBP appear to agree remarkably well during the 20th century. Not only does NBP stay close to zero (as it should, assuming that primary production and the losses of carbon due to turnover, mortality, decomposition and disturbances are "in natural balance"), but also the interannual variations simulated by both models are highly correlated. This agreement reflects the level of calibration and testing applied to both models when validated against observed measurements and forced by 20th century observed climate data. However, when projected into the future, small differences in simulated annual NBP accumulate causing the two models to diverge significantly around 2025-2030. This divergence occurs because the simulated NBP is a small difference between two relatively large and opposing fluxes. Evidently the models differ very significantly in their representations of NPP and also in the ways they treat decomposition and disturbance effects.

² Area-weighting here means the values obtained for every grid cell were corrected for the actual grid cell area (varying approximately as the cosine of the latitude of its centroid) before aggregation at the continental scale.

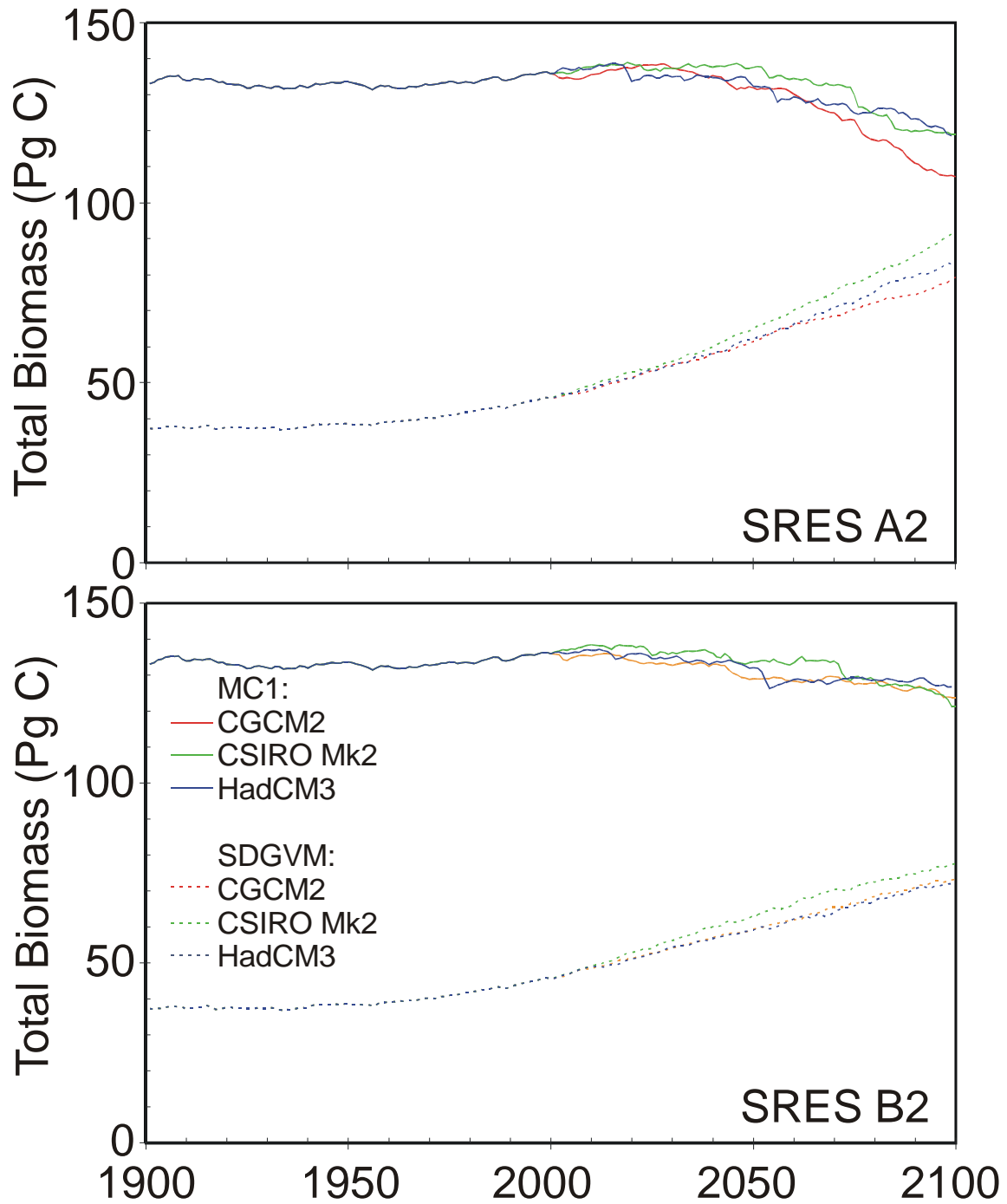


Figure 7. Time series of total vegetation biomass for Canada and the continental USA (i.e., including Alaska), as simulated by the MC1 and SDGVM dynamic vegetation models. Data for the 20th century were obtained using observed climate and CO₂ forcing, and for the 21st century using different GCM scenarios of future climate and SRES CO₂ emissions scenarios. Top: SRES A2 projections; Bottom: SRES B2 projections. Data are reported at annual intervals, aggregated up from approximately 10,000 grid cells with area-weighting. 1 Petagram, Pg = 10¹⁵ gram = 1 Gigatonne.

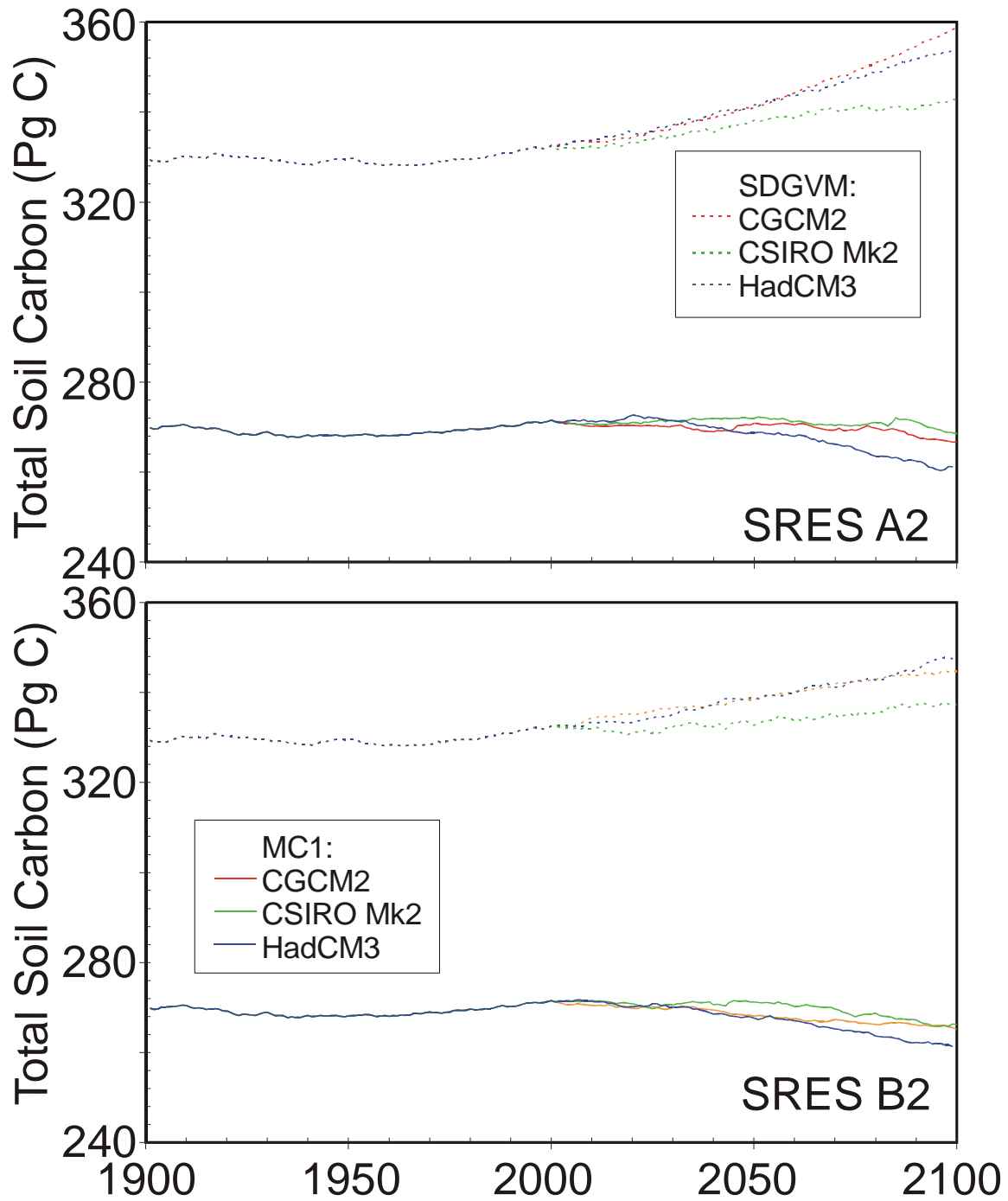


Figure 8. Time series of total soil carbon for Canada and the continental USA as simulated by the MC1 and SDGVM dynamic vegetation models. Data for the 20th century were obtained using observed climate and CO₂ forcing, and for the 21st century using different GCM scenarios of future climate and SRES CO₂ emissions scenarios. Top: SRES A2 projections; Bottom: SRES B2 projections. Data are reported at annual intervals, aggregated up from approximately 10,000 grid cells with area-weighting.

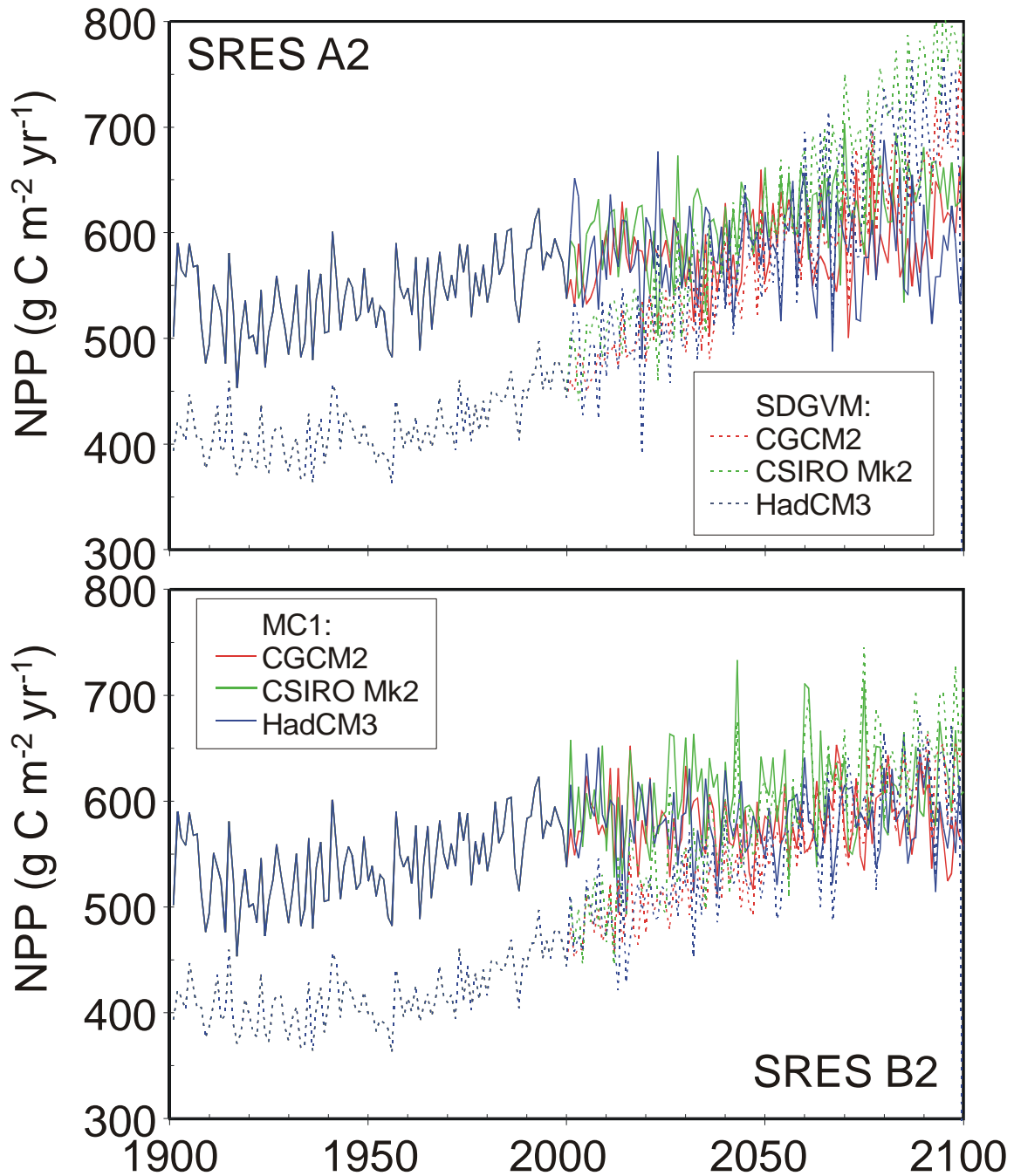


Figure 9. Time series of total net primary production (NPP) for Canada and the continental USA as simulated by the MC1 and SDGVM dynamic vegetation models. Data for the 20th century were obtained using observed climate and CO₂ forcing, and for the 21st century using different GCM scenarios of future climate and SRES CO₂ emissions scenarios. Top: SRES A2 projections; Bottom: SRES B2 projections. Data are reported at annual intervals, aggregated up from approximately 10,000 grid cells with area-weighting.

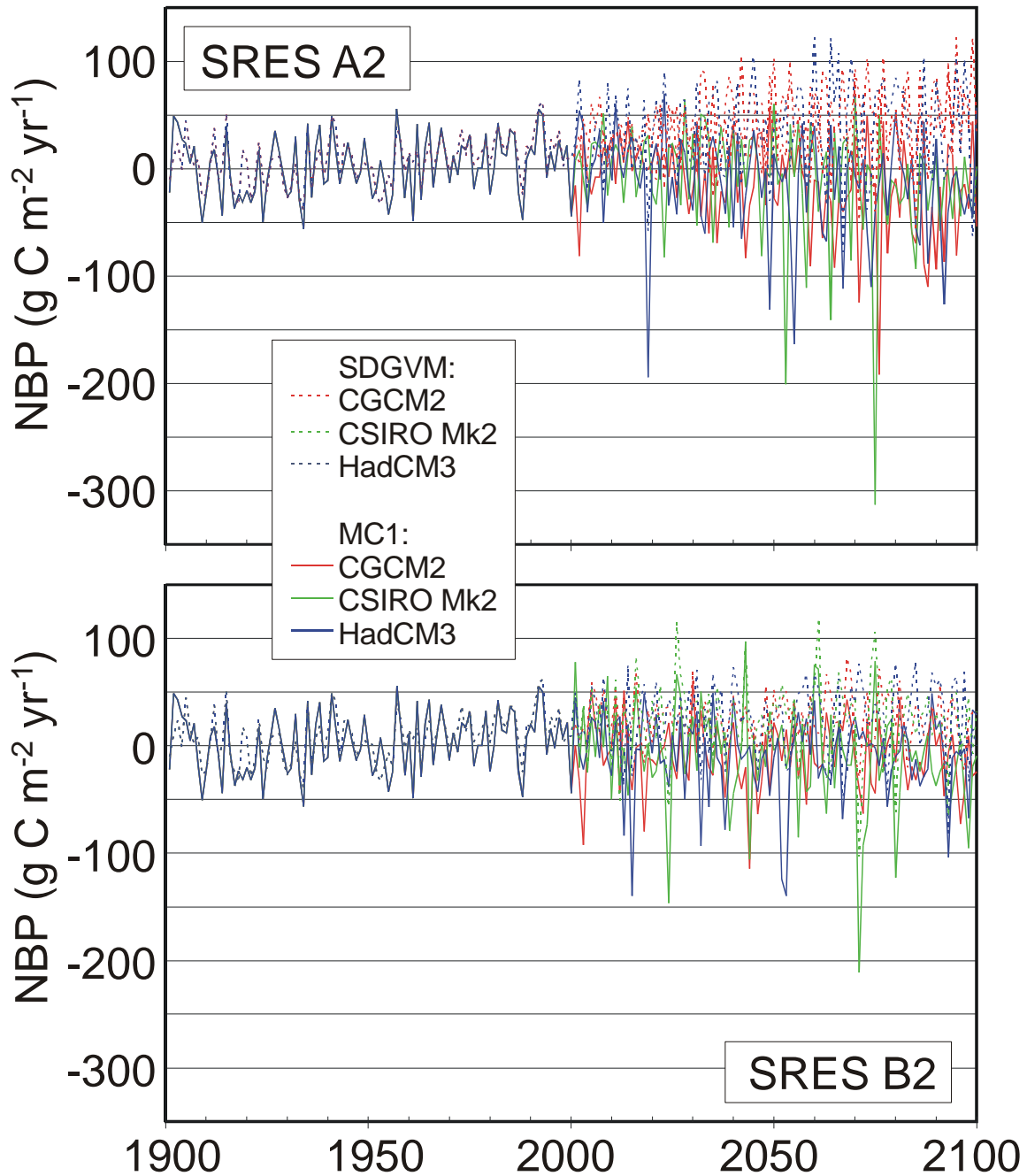


Figure 10. C Time series of total net biome production (NBP) for Canada and the continental USA as simulated by the MC1 and SDGVM dynamic vegetation models. Data for the 20th century were obtained using observed climate and CO₂ forcing, and for the 21st century using different GCM scenarios of future climate and SRES CO₂ emissions scenarios. Top: SRES A2 projections; Bottom: SRES B2 projections. Data are reported at annual intervals, aggregated up from approximately 10,000 grid cells with area-weighting.

Each model produces remarkably similar responses in NPP and NBP to historical climate fluctuations. Even in the future climate scenarios it is possible to detect covariance of the two models when forced by the same scenario, but in Figures 9 and 10 this is obscured by differences in the timing of climatic “events” simulated by the different GCMs. It is even difficult to distinguish clear differences between the A2 and B2 emissions scenarios. It seems clear, however, that the explanation for these different responses lies in the different assumptions built into each model. Figures 11 and 12 show the spatial distributions of NPP as simulated by each model for the historical period (represented by the year 2000) as well as for each of the six future climate projections (represented by the year 2100, or 2099). Note that in these maps, as well as those shown in Figures 13 and 14, the data are actually 10-year averages for the decade prior to the year shown. This averaging was needed to reduce the effects of interannual variability which could otherwise obscure some of the underlying spatial similarities. Here some regional differences among the different climate scenarios are visible, but the differences between the two DGVMs are still much greater. In the 20th century, MC1 tends to predict higher NPP in many regions, notably the US eastern seaboard, the tundra immediately north of the Canadian boreal region, the Pacific Northwest coast, and southwestern Alaska. SDGVM, though generally reporting lower productivity is more uniform and slightly higher in most of the boreal region. For the 21st century, SDGVM shows major increases in NPP over most of the continent under all six scenarios, notably in the southeastern USA. In general the A2 scenarios produce greater increases, with even the southwestern USA projected to improve slightly in spite of the present-day aridity. MC1 generally projects decreases in NPP although it appears to be more sensitive to the different GCM scenarios. The common story seems to be that areas of relatively low precipitation, including the western boreal and Arctic, are subject to major reductions in NPP, tending to zero, with variable responses (including modest increases as well as decreases) in the USA and southern Canada.

Figures 13 and 14 then show simulations of net biome productivity (NBP) for the two models. Here the general spatial distributions are fairly similar for 2000, but MC1 shows greater variability, with remarkably negative NBP in central Alaska. This is evidently due to the more stochastic properties of MC1’s forest fire model, as compared to the average annual area burned approach followed in SDGVM. For the 21st century, the divergence previously noted in the time-series graphs (Figure 10), is reflected in both the relative magnitudes of changes and their spatial distributions. MC1 projects some major decreases in eastern Canada (CGCM2 and CSIRO Mk 2), and south eastern USA (most GCMs), with increases in the western and central USA. Some very negative NBP values occur across southern Canada and into the eastern USA. These can be attributed to the greatly increased fire activity projected in these regions by MC1. In comparison, SDGVM projects some significant decreases in the southern USA (notably with CSIRO and Hadley A2 scenarios, but particularly HadCM3) and in central Canada under CSIRO Mk 2 B2, with little change or increases elsewhere.

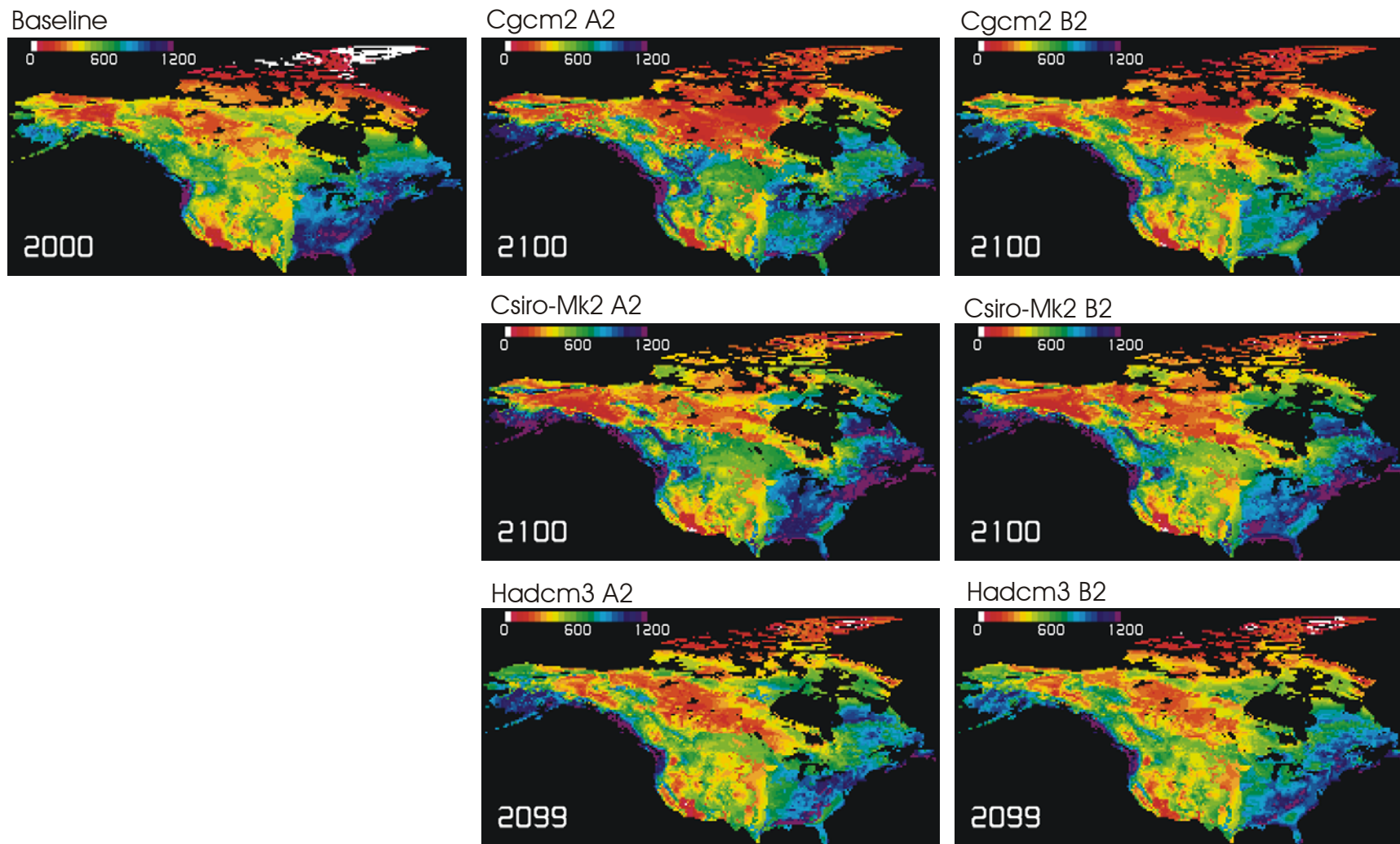


Figure 11. Changes in annual average net primary productivity ($\text{g C m}^{-2} \text{ yr}^{-1}$) as simulated by MC1 for the decades 1991-2000 and 2091-2100 under each of the six climate scenarios.

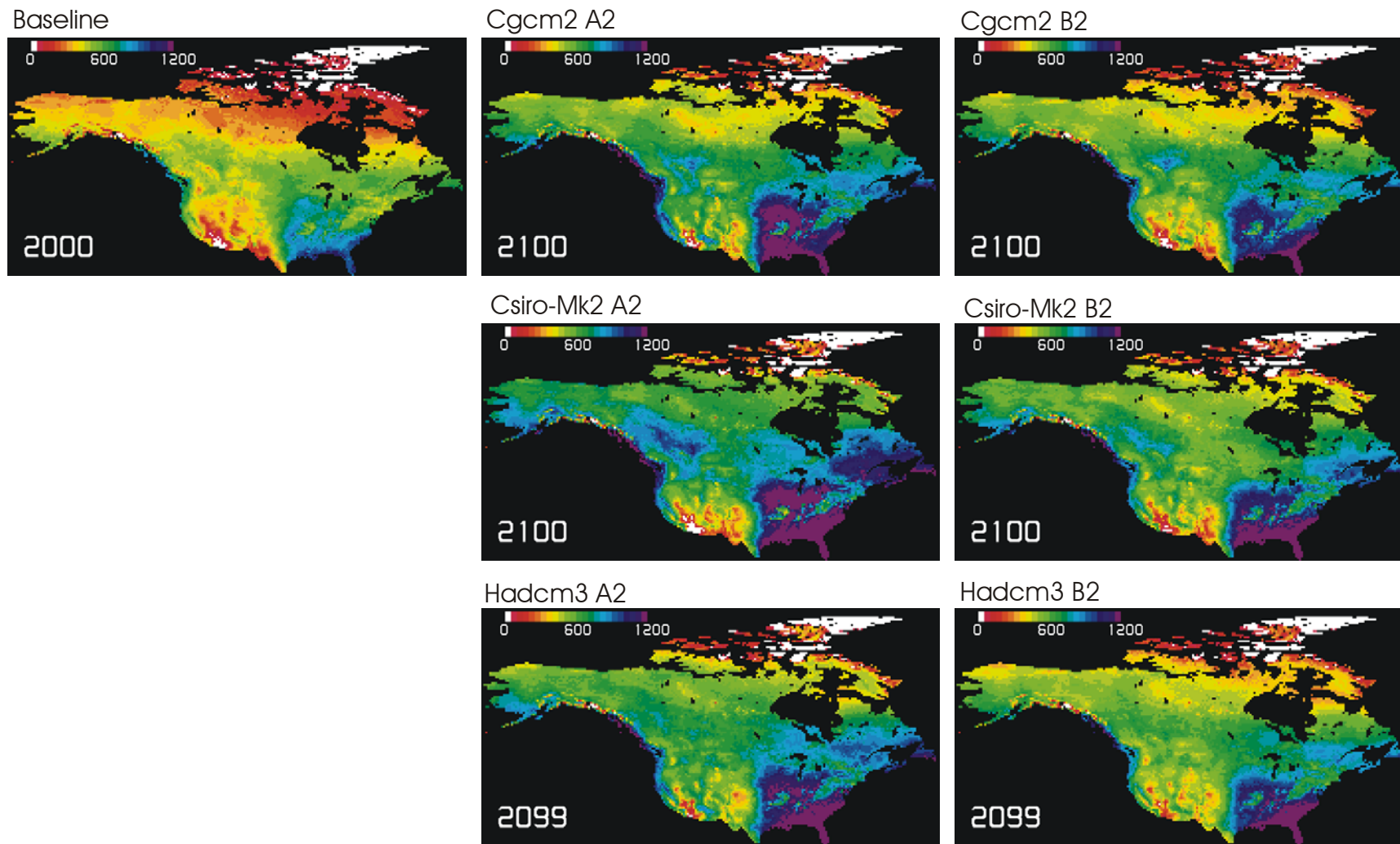


Figure 12. Changes in annual average net primary productivity ($\text{g C m}^{-2} \text{ yr}^{-1}$) as simulated by SDGVM for the decades 1991-2000 and 2091-2100 under each of the six climate scenarios.

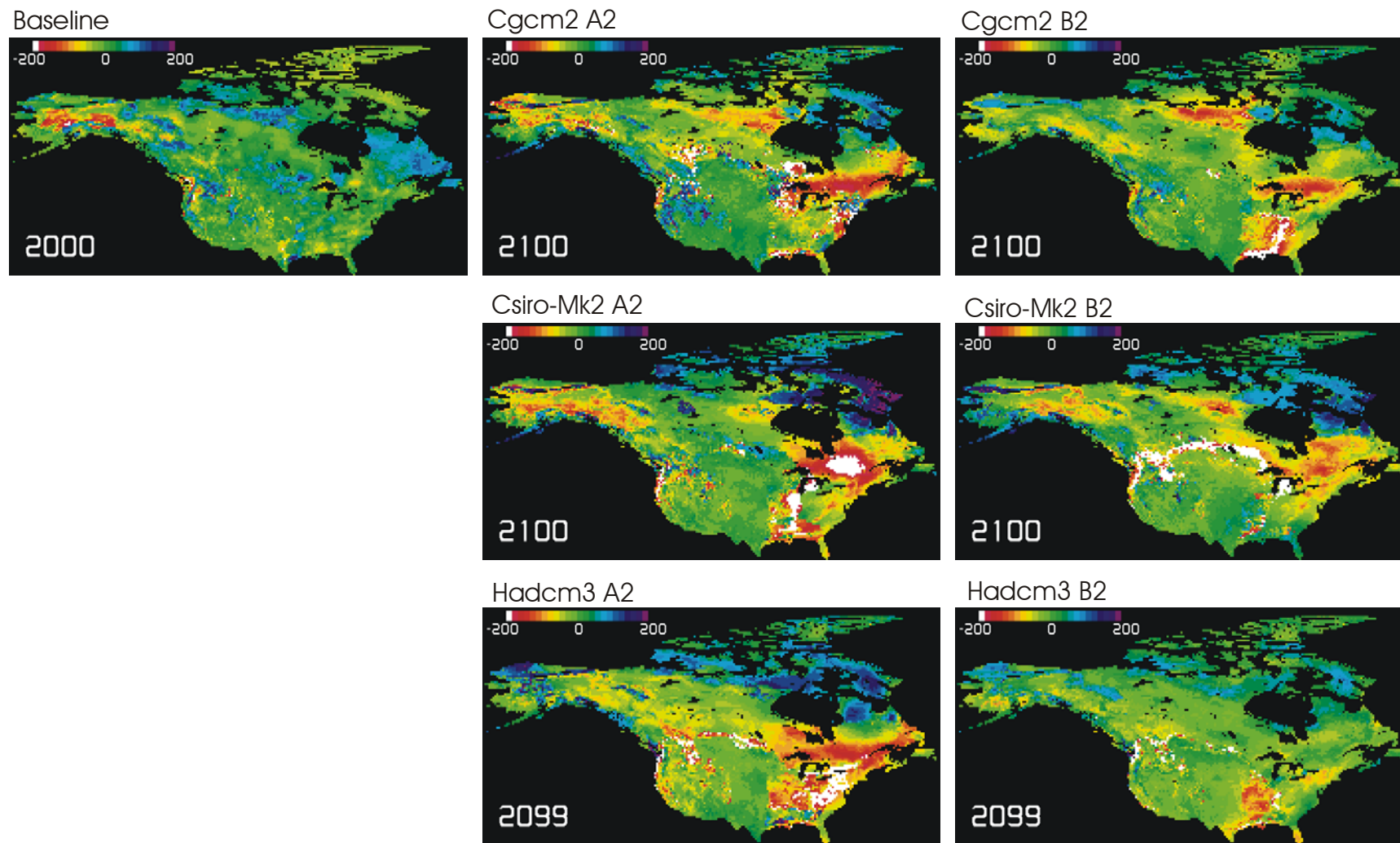


Figure 13. Changes in annual average net biome productivity ($\text{g C m}^{-2} \text{ yr}^{-1}$) as simulated by MC1 for the decades 1991-2000 and 2091-2100 under each of the six climate scenarios. Note the very negative values seen in southern Canada for the Hadley and CSIRO scenarios.

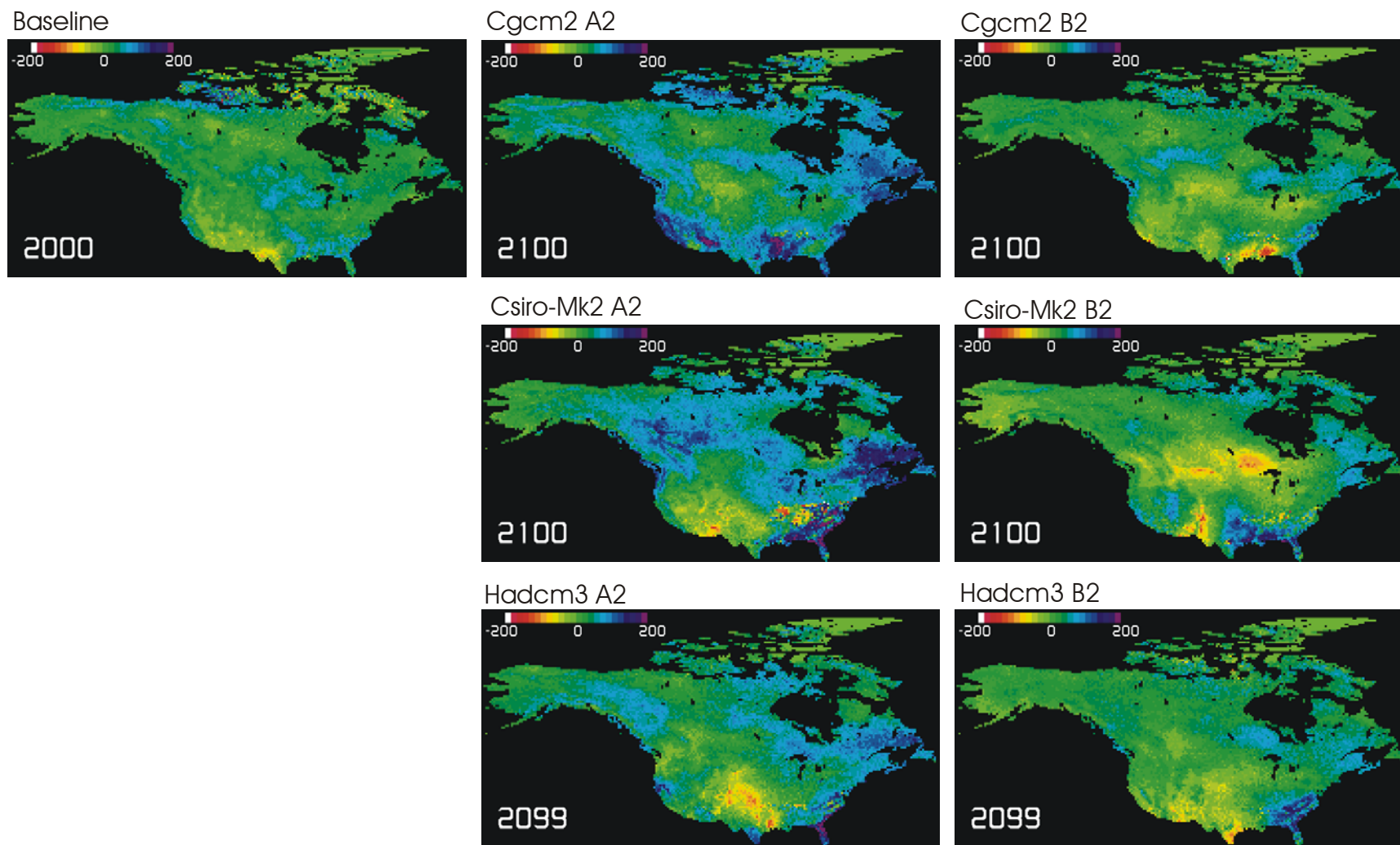


Figure 14. Changes in net biome productivity ($\text{g C m}^{-2} \text{yr}^{-1}$) as simulated by SDGVM for the decades 1991-2000 and 2091-2100 under each of the six climate scenarios.

Figure 15 shows major vegetation zones as simulated by MC1 for 2000 and as projected to change by 2100. It should be noted that comparable data were not available from the SDGVM simulations. There are differing views on the value of predicting vegetation distribution using a DGVM. On the one hand, it has been argued that a model that can successfully recreate the observed vegetation in a particular region is meeting a stringent requirement in verifying model performance: “correct” values for other indicators such as areal evapotranspiration, NPP and densities of carbon in vegetation and biomass, have little significance unless they are coupled with observed vegetation types. The alternative view is that the classification of vegetation (based on simulated structural attributes such as leaf area index (LAI) and biomass density of different plant functional types) is as much art as science, so that it is possible to produce credible vegetation maps from simulations that are otherwise demonstrably poor! The authors support the former viewpoint. MC1 is fairly successful in capturing the broad distributions of observed biomes in North America, although some of the details are clearly wrong. For the future, MC1 projects several changes under all the GCM scenarios (similar to those obtained from the IBIS projections for Canada shown in Figures 3 and 4). These include northward expansion of tundra and boreal regions into the Arctic and the loss of forest to grasslands, particularly in the prairie regions. In the USA, common trends appear but the areal extents and types of vegetation that replace the “present-day” ecosystems are variable. For example, in the southeast, present-day temperate deciduous, cool temperate mixed, and warm temperate/subtropical forest types give way to differing extents and distributions of savanna type ecosystems, leaving some of the existing vegetation in some cases (CSIRO Mk2, CGCM2 B2 and HadCM3 A2) and relatively little in others. Recognizing the limitations in these simulations, the implications of projected changes in vegetation distribution for protected area system planning and conservation policy (e.g., see Suffling and Scott 2002; Scott et al. 2002) are being examined in a graduate thesis in the Faculty of Environmental Studies at the University of Waterloo.

Figures 16-19 present the simulation results for spatial distributions of biomass and soil carbon corresponding to Figure 11-14. As noted previously from Figures 7 and 8, MC1 typically overestimates biomass C density for much of Canada, where observed densities may be as little as 25% of the simulated values, particularly in northern Québec, the Territories and the Prairie Provinces (e.g., see CFS CanFI-based estimates of forest biomass reported by Penner et al. 1997). SDGVM on the other hand typically predicts values around 25% of those obtained from MC1, even in regions of the USA where higher densities would be expected (though it is difficult to be precise because spatially detailed US forest biomass data comparable to those derived from CanFI data were not available). Hence, SDGVM appears to be a lot closer to reality in its estimates of typical vegetation carbon densities, and may even tend to underestimate. Consistent with SDGVM’s projections of increasing NPP and NBP, the future projections show significant increases across the continent, even including the western USA which shows almost zero biomass in 2000 for most of the desert and mountain States. Responses are particularly pronounced along the eastern seaboard, and particularly under the warm wet CO₂-rich CSIRO Mk 2 A2 scenario. These responses contrast markedly with those projected by MC1 which projects major declines in the southeastern USA and some decreases in the southern Canadian boreal, compensated by increases for much of eastern

Canada and some parts of the far north. These results must be taken with caution. First, MC1 already overestimates biomass C for much of Canada, and even after some major declines are forecast across the USA, it still projects double the average biomass projected by SDGVM for 2100 (see Figure 7). Second, much of the projected increases, e.g., in northern Québec, are in regions where present-day soils are shallow and/or undeveloped, so are unlikely to be able to support major vegetation growth in the near future (even assuming regeneration could be achieved).

Figures 18 and 19 show the differences in soil carbon distribution as simulated by the two models. At first sight SDGVM predicts more soil C than MC1 mainly in the north, where the landscape is varied and major forest fires have had a major impact. The SDGVM map for 2000 shows relatively little spatial variation (and even more so for all the GCM scenarios in 2100). Available data however suggest that both models may be underestimating soil carbon accumulations quite significantly, particularly in Canada and Alaska. Data from global soil carbon maps (e.g., <http://soils.usda.gov/use/worldsoils/mapindex/soc.html>) indicate some organic C densities greater than 100 kg C m^{-2} while the more detailed North American Soil Organic Carbon map of Lacelle et al. (1997) shows areas south of Hudson Bay and around the Canada/Alaska border, where total organic C densities exceed 200 kg C m^{-2} , compared to maximum values simulated by SDGVM of about 20 kg C m^{-2} . To some extent, these differences may be due to both models not explicitly simulating organic soils.

Given the importance of fires in the boreal zone, this may reflect SDGVM's comparatively simplistic fire model. With the GCM scenarios, the variability is further reduced, presumably because generally increasing NPP allows the less productive regions to catch up, while those simulated ecosystems that had already developed high soil C densities are closer to equilibrium of litter production and decomposition. On the other hand, although MC1 does not project much less soil carbon (and most of the difference is contained in its higher biomass estimates), it is missing large areas in northern Canada and Alaska where one might expect organic material to accumulate. However, MC1's responses of these regions to the climate scenarios seem very reasonable: soil C stocks are generally depleted, particularly with the "warm-dry" CGCM2 scenarios.

A series of simulations was also carried out with MC1 to investigate the effects of fire suppression as an adaptation to climate change effects. Fire suppression was not considered in SDGVM however, and therefore a comparison between two DGVMs was not possible. Moreover, the great disparity in the results obtained from the two models for unsuppressed fire suggests that there are more fundamental questions related to model refinement is needed before we can consider whether the effects of simulated fire suppression are reasonable.

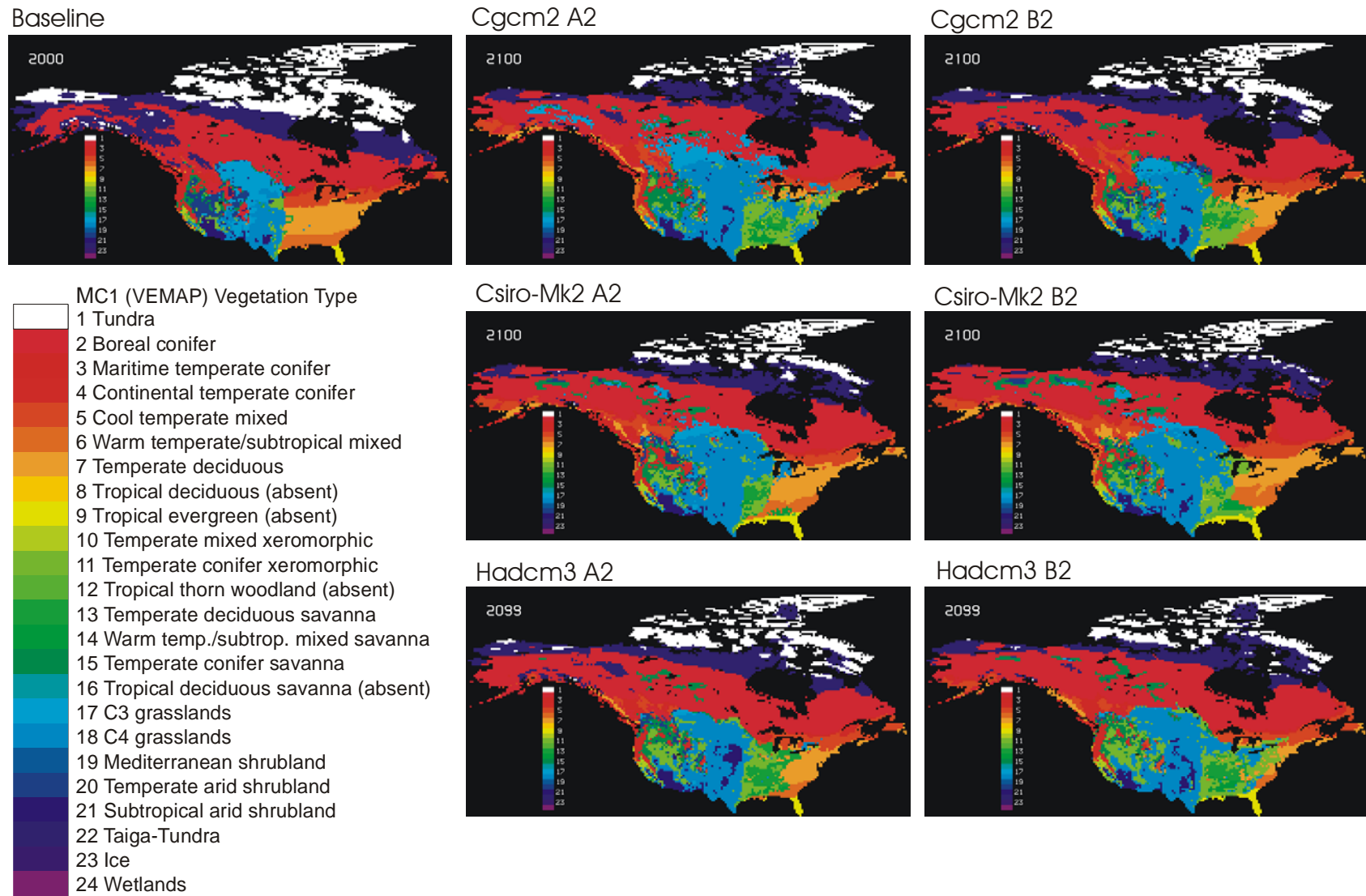


Figure 15. Changes in dominant vegetation types as simulated by MC1 for 2000 and 2100 under each of the six climate scenarios. The classification legend follows that of VEMAP.

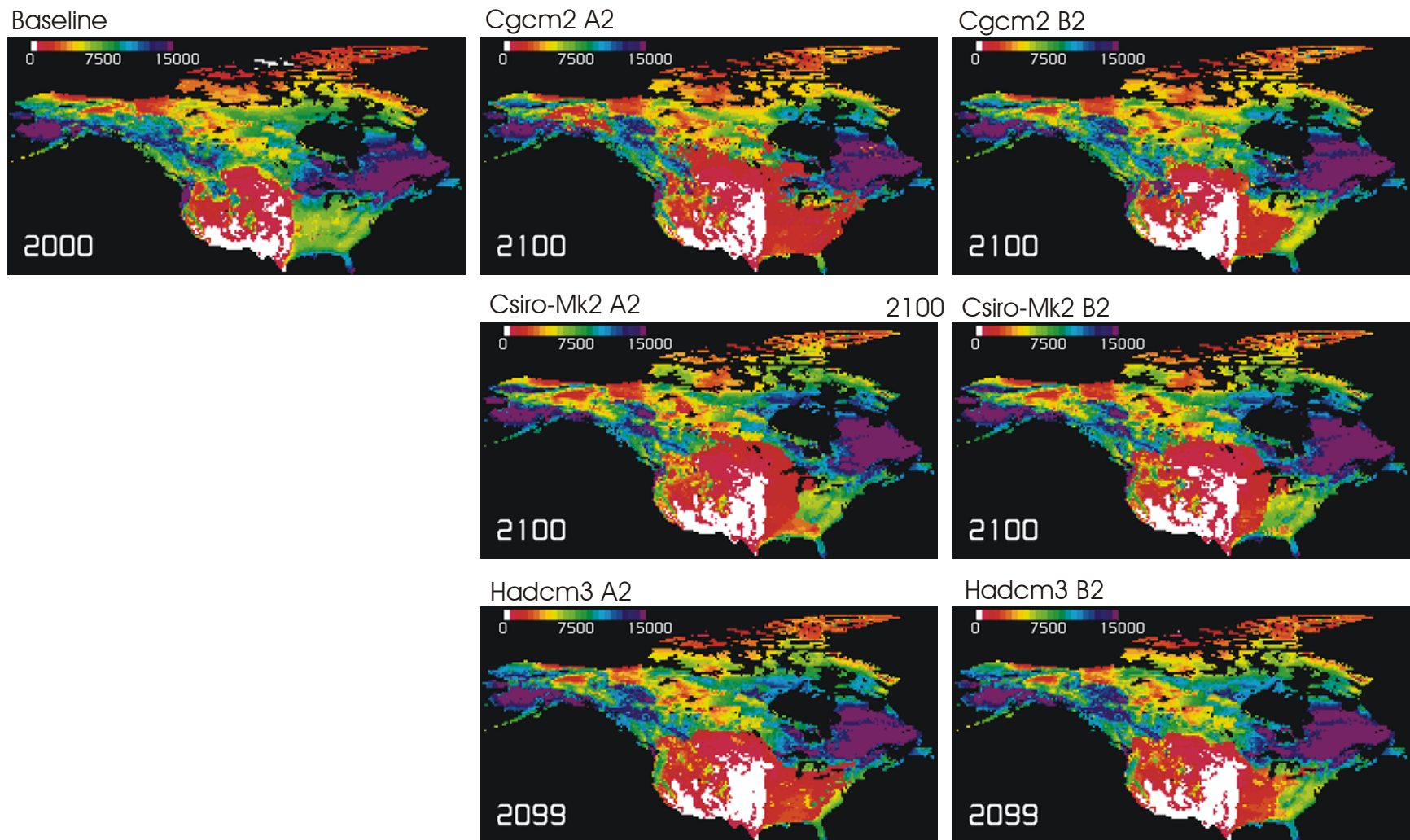


Figure 16. Changes in total vegetation carbon density (g C m^{-2}) as simulated by MC1 for 2000 and 2100 under each of the six climate scenarios.

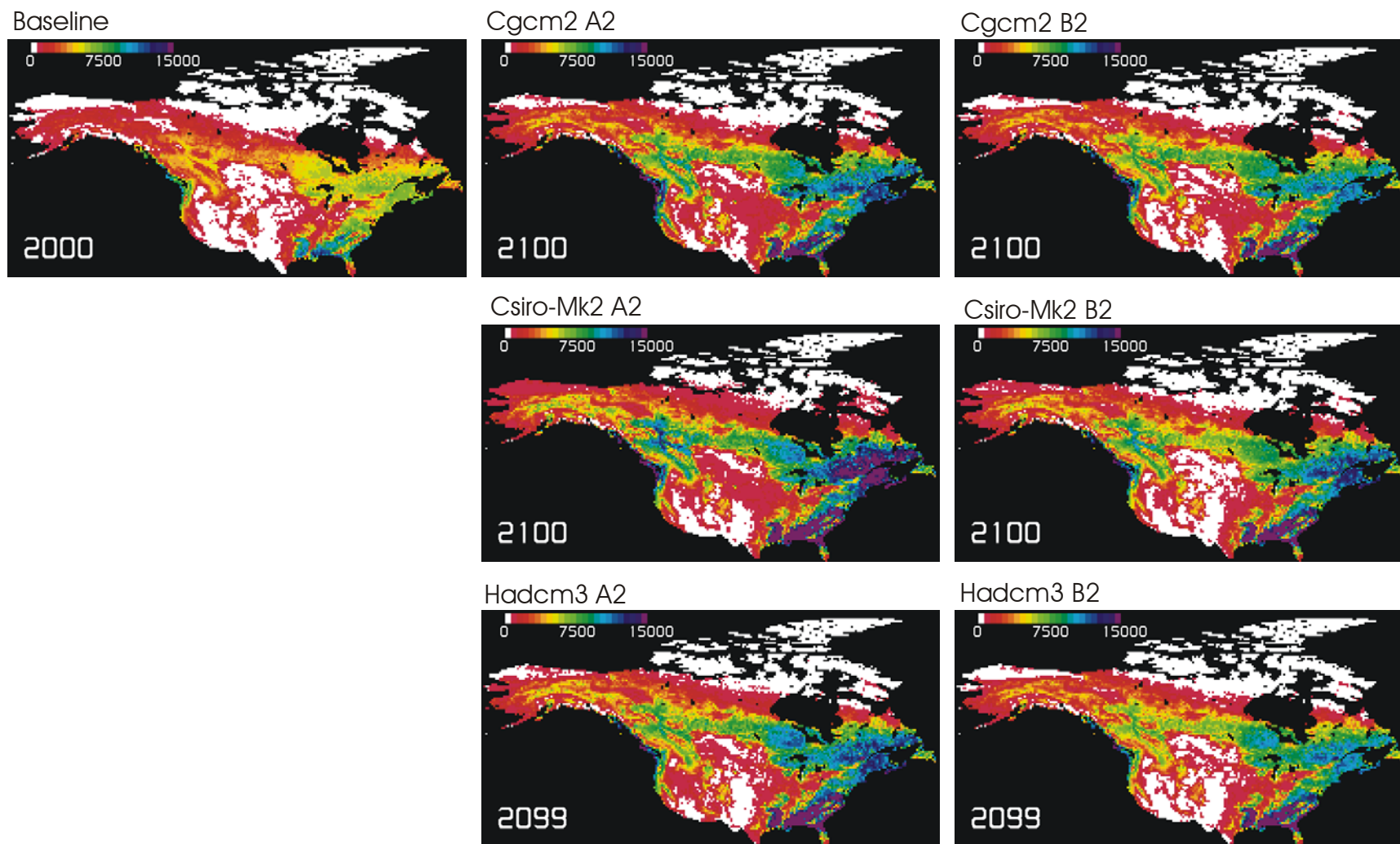


Figure 17. Changes in total vegetation biomass density (g C m^{-2}) as simulated by SDGVM for 2000 and for 2100 under each of the six climate scenarios.

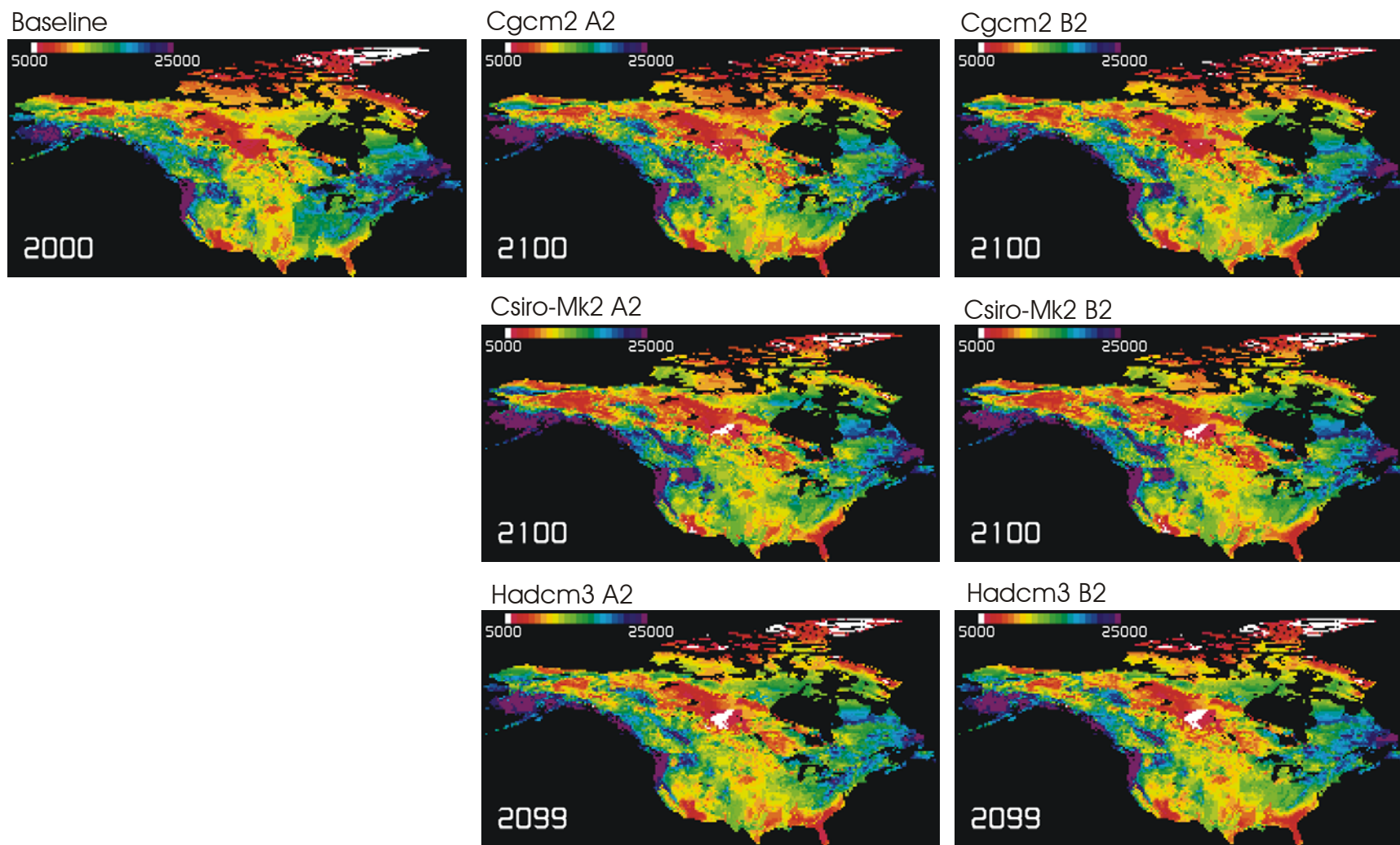


Figure 18. Changes in total soil carbon density (g C m^{-2}) as simulated by MC1 for 2000 and 2100 under each of the six climate scenarios.

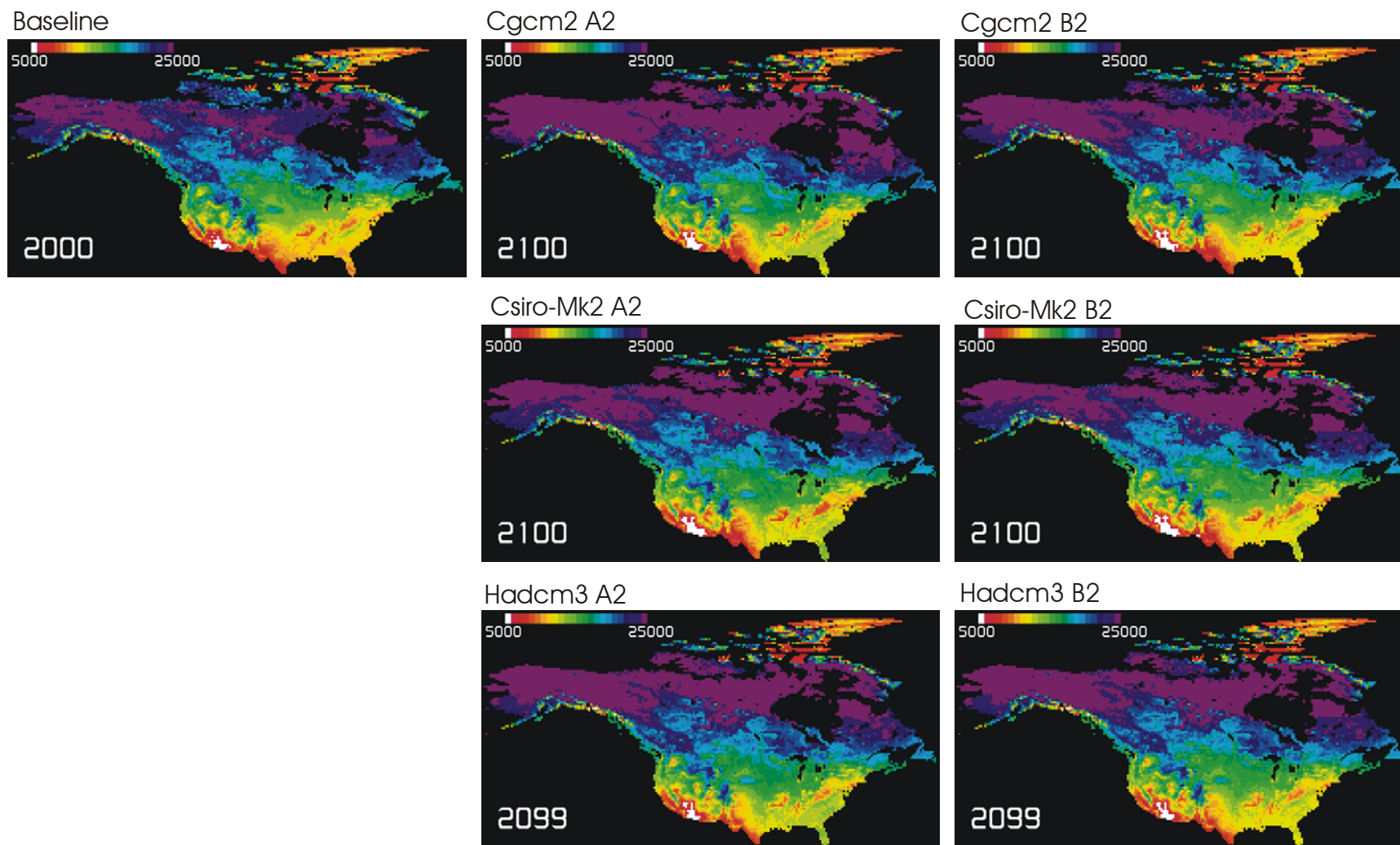


Figure 19. Changes in total soil carbon (g C m^{-2}) as simulated by SDGVM for 2000 and for 2100 under each of the six climate scenarios.

5 Discussion

A principal finding of this model inter-comparison project was that the differences in the results obtained from the two DGVMs are substantially greater than the differences resulting from the range of climate forcings produced by each of three GCMs (Canadian CGCM2, UK HadCM3 and Australian CSIRO Mk. 2) and two IPCC SRES emissions scenarios (A2 and B2). This result does not invalidate all comparisons of the impacts of the different climate scenarios on North American forests, but it does suggest that further investigation of the models is required, at least until there is enough evidence to reject the results from one of them because of a clear error or weakness. The following discussion focuses on these model differences.

In essence, the divergence between the two DGVM projections shows SDGVM responding with increases in many key ecosystem indicators (biomass carbon, total carbon, NBP, and NPP), whereas MC1 shows an initial increase in NBP (albeit somewhat slower, because of lower sensitivity of NPP to increasing CO₂ concentration, see below), followed by a serious decline from about 2030 onwards. By 2100 these projected changes in NBP lead, on the one hand, to significant gains in biomass carbon and total ecosystem carbon when simulated by SDGVM, but to major losses when simulated by MC1 (with the CGCM2-A2 climate scenario causing the biggest declines). Neilson et al. (2006) have described these as the “green-up” and “green-up followed by brown-down” projections, respectively. It should be noted that several of the major differences between the two models are clearest when they are driven by the CGCM2 A2 scenario, because of the greater CO₂ forcing and because CGCM2 is typically the “driest GCM” for most regions of North America (i.e., relatively large increase in temperature combined with relatively small changes in precipitation).

The MC1 projections show the greatest carbon losses occurring in three major forested regions of North America, broadly grouped by Neilson et al. (2006) as western USA, eastern USA and the boreal (covering Alaska and much of western and central Canada). It is worth noting that the earlier (unpublished) IBIS simulations for the western Canadian boreal region are consistent and also projected significant declines in forested cover (Figures 3 and 4) and total biomass carbon (Figures 5 and 6), when driven by the CGCM2 IS92A scenario (which closely resembles the CGCM A2 used in VINCERA).

The evident disparity between SDGVM and MC1 has led to a critical examination of the underlying assumptions in the two models, mainly by Ron Neilson’s group, and the investigation continues. In many ways the models are similar, but there are some key differences. First, photosynthetic response to increasing CO₂ is simulated in SDGVM using the Farquhar model but using the empirical *beta factor* approach in MC1. The consequences of this difference are clearly seen in Figure 9, where NPP simulated by SDGVM is initially lower but increases more rapidly with time (i.e., due mainly to increasing CO₂ concentration). In subsequent experiments, Neilson has found it is possible to make the two graphs agree very closely by halving the SDGVM’s CO₂ sensitivity or doubling that of MC1.

The MC1 team has also compared both models' responses to increased CO₂ concentration with observations of CO₂ responses reported recently by Norby et al. (2005) for forested Free-Air CO₂ Enrichment (FACE) experimental sites. The observed responses average about 23% increase in NPP for a notional doubling of pre-industrial concentrations (275 to 550 ppm), which are actually very consistent with those predicted by SDGVM using the Farquhar model. In personal communications, Neilson and Norby are agreed that all FACE experiments at forested sites have a common major limitation in that none of the stands growing in elevated CO₂ have reached the inflection point on their growth curves. I.e., they cannot be considered to have approached the carrying capacity of their respective sites. One view is that stands approaching maturity will inevitably slow down, so that at stand culmination, total biomass accumulation will be essentially no greater than that of a stand growing at present-day or historical CO₂ levels. [From a forest management perspective, this positive CO₂ fertilization effect suggests a possible adaptation opportunity, because (assuming no negative impacts of a warmer climate) stands managed on short rotations (e.g., willows and poplars) would presumably receive a significant "lift" from CO₂ fertilization.]

The second major difference in the two models is that SDGVM simulates fire effects using an average area burned per year, which shows very little change in response to climate (either historically or under the different climate scenarios), whereas MC1 (reflecting its origins in the US Forest Service), has a much more detailed and responsive representation based on US and Canadian Fire Weather Indices, including effects on fuel build-up and flammability. Therefore, one might guess from the latter difference that MC1's greater sensitivity to fire would explain the ultimate brown-down result, but this is not so, because in fact SDGVM actually burns *on average about three times the area* per year. The explanation for the difference appears to lie mainly in the simulated vegetation response to hot dry years. In SDGVM, the increasing NPP simulated in response to increasing atmospheric CO₂ also drives a further increase in canopy water use efficiency (WUE). It appears that this increase in WUE allows the simulated vegetation to respond positively, even in warm dry conditions, offsetting increases in area burned and in soil and litter decomposition rates. With MC1, however, the increase in WUE is directly proportional to the increase in NPP simulated using the beta factor, which is approximately 50% of that predicted by SDGVM. Increased evaporative demand after 2030 causes the vegetation to become seriously drought stressed over extensive areas in many years, causing widespread reductions in leaf area and increased mortality. To some extent these losses are correlated to increased fire occurrence in simulated by MC1 in drier years, which may be due to earlier drought stress causing increased fuel build-up. In some cases, the simulated fires may trigger replacement by less productive vegetation types—all of which add to the "brown-down" phenomenon.

The higher rate of disturbance simulated by SDGVM may also prevent stand growth from ever reaching carrying capacity, leading to lower biomass densities than observed even as climate change and increasing CO₂ contribute to increasing disturbances and productivity (the net effect being that NBP remains positive). MC1 on the other hand, has a much more detailed forest fire model, with the consequence that areas with higher biomass and more litter (fuel) accumulation are disturbed more frequently, and release much greater amounts of carbon. MC1 also greatly exaggerates

forest biomass accumulation (i.e., trees grow more slowly, but they live longer!). It should be noted that MC1 does a credible job of predicting North American vegetation zones, but SDGVM does not currently attempt this challenging aspect of simulating vegetation.

Neilson (personal communication, 2006) also suggests tentatively that one of the key factors causing the differences in simulated drought responses between MC1 and SDGVM lies in their respective handling of soil water storage. Some global scale models, including IBIS, grossly exaggerate soil depth (to allow realistic simulation of high transpiration rates seen in tropical ecosystems). This could generate very misleading results in many temperate and boreal forested regions where undeveloped soils, particularly at high elevations and/or high latitudes (e.g., Canadian Shield) may in reality store very little water. Unfortunately, SDGVM's treatment of soil hydrology is not well-documented. With the relatively limited data available on soil water holding capacity at continental scale (particularly in Canada), it is unclear how serious this problem may be, though we tried to address this problem with the development of the NAGSOIL data set.

Hence an explanation for the differences between the two models may be that the relatively high annual area burned in SDGVM contributes to lower average biomass, while its greater positive response of NPP and WUE to increasing CO₂ concentration allows NBP to stay positive. In addition, however, SDGVM must be transferring more of its higher productivity into the soil pool in order for NBP to stay positive. Evidently, warmer conditions are not accelerating its loss of soil C (which ramps up through 2100, while MC1 shows a slight but continual decline). On the other hand, MC1 accumulates more C in biomass, which is then available for mortality, decomposition and burning. The differences in litter production or in organic matter decomposition would only need to be slight to contribute to major differences in the long-term carbon balance. It is difficult to say whether this interpretation is correct, and if so which model is more valid.

These results raise some important questions that cannot be answered directly, and indicate key areas for future research:

1. Will positive growth responses of forest stands to increased CO₂ be sustained as stands approach maturity and productivity becomes more constrained by site conditions and competition?
2. Although it seems clear that a warmer climate will generally be a drier climate, what will be the likely responses of forest stands operating at higher water use efficiency? Under what circumstances will the negative effects of increased evaporative demand outstrip the benefits of increased CO₂?
3. What are the likely consequences of drought stress on mortality and litter production, and on the interactions with fire and other disturbances?
4. A further complication raised by question 2 (and by the disparity of the results obtained from SDGVM and MC1) suggests that we need to better understand the role of soil hydrology as a factor influencing site water balance at the large scale. This is coincident with one of the problems that Price et al. have encountered with IBIS. It suggests that we need a better national scale mapping of soil texture and depth, and other hydrological properties, particularly for non-agricultural regions.

The modelled continental scale estimates of total biomass and soil carbon stocks and of annual mean NBP and NPP can be compared to other estimates derived from measurements. North American woody biomass carbon stocks have been estimated for 1995-1999 as 23–26 Pg C (Myneni et al. 2001), suggesting that both models are overestimating, though SDGVM is much closer to the reported values (about 45 Pg C during 1990-2000, Figure 7). Continental scale estimates of soil carbon are difficult to locate: Lacelle et al (1997) estimate total soil organic carbon for USA and Canada as about 335 Pg C, but this includes peatlands. There do not seem to be any continental-scale estimates of the stock of inorganic soil C. Presumably it is a small fraction of the organic C stock, in which case, Figure 8 shows both DGVM estimates are close, with approximately 270 Pg C for MC1 and 330 Pg C for SDGVM!

Modelled values of NPP are difficult to compare with observations, though both models appear to give values consistent with expectations when averaged over a complete range of sites and climatic regions. In comparison NBP is relatively well documented. Over the 100 years from 1901 to 2000, MC1 estimated mean annual NBP of $\sim 47 \text{ Tg C yr}^{-1}$ compared to about 150 Tg C yr^{-1} estimated by SDGVM³. The latter estimate is very comparable to recent estimates of North American C budget based on “tall-tower” measurements of large-scale CO₂ fluxes (Jing Chen 2006, pers. comm.). Recent work of Kurz et al. and Chen et al. has shown general convergence on Canada currently (ca. 2000) being a small C sink of approximately 50 Tg C yr^{-1} , which might suggest that the estimates reported here are not particularly reliable. However, it should be noted that the analyses for the 20th century carried out by these researchers are based on observations including forest inventory data (CBM-CFS, Kurz and Apps 1999) and records of areas lost to disturbances, primarily fires, based on a combination of inventory data, fire records, and satellite imagery in recent decades (BEPS-InTEC, e.g., Chen et al. 2003). Disturbances are affected by decadal-scale fluctuations in climate contributing to effects on forest age-class structure and thus contribute significantly to inter-decadal scale variations in NBP. These effects are captured to a large extent by the models of Chen et al. and Kurz et al.

In comparison, the DGVM simulations reported here are “unconstrained estimates”, meaning they did not depend on observed data on disturbance history, forest inventories or satellite imagery to determine when and where disturbances should occur. Only the observed climate history was used to drive the disturbance events simulated in each model. It is rather unlikely that the timing and location of these simulated disturbances would correlate very strongly with observed areas disturbed (particularly when considering the effects of fire suppression which has been carried out at some level for much of the continent from about 1920 onwards), and hence a close correlation cannot be expected between annual NBP estimated by the DGVMs and that estimated from available data. It therefore follows that estimates of continental-scale annual NBP should be compared over periods of several years or even decades; in this regard, both models are performing quite well. Moreover, the lower estimates from MC1 could be related to two factors: (1) approximately 100 grid cells were not simulated where soil types were predominantly organic, which may contribute to an underestimation of NBP

³ One Teragram, Tg = 10^{12} g = 10^6 metric tonne. One Petagram, Pg = 10^{15} g = 10^9 metric tonne.

(though this is unlikely to have a large impact because productivity in these few grid cells would likely be low); and (2) fire suppression effects were not simulated even though it is generally accepted that areas burned over much of North America have been reduced significantly during the 20th century due to fire management and suppression practices.

6 Acknowledgements

Major funding for this project was provided by the Government of Canada's Climate Change Impacts and Adaptation Program. Additional resources came from Natural Resources Canada internal allocations and from the Panel on Energy Development (PERD) Program at Objective Level 6.2.1. Within the Canadian Forest Service, Pia Papadopol, Marty Siltanen, Fred Woslyng and Travis Logan (now with Ouranos in Montreal) all contributed substantial effort in preparing and managing input data sets and in creating output files for presentation. Ray Drapek of Forest Sciences Laboratory at Oregon State University similarly provided much help in comparing and validating our data sets with those from VEMAP. DTP also acknowledges many suggestions and coding fixes for IBIS contributed by Mustapha El Maayar at University of Toronto, Department of Physical Geography. Ron Stouffer at GFDL gave us access to historical and IPCC SRES scenario CO₂ concentration time-series data. Hans Luthardt of the IPCC Data Distribution Centre provided temperature data from the European Community ECHAM4 GCM, and Tony Hirst of CSIRO Division of Atmospheric Research made temperature and humidity data available from the CSIRO Mark 2 GCM archives.

7 References

- Bachelet, D., R.P. Neilson, T. Hickler, R.J. Drapek, J.M. Lenihan, M.T. Sykes, B. Smith, S. Sitch and K. Thonicke. 2003. Simulating past and future dynamics of natural ecosystems in the United States. *Global Biogeochemical Cycles* **17(2)**: 1045-1065.
- Chen J.M., W. Ju, J. Cihlar, D.T. Price, J. Liu, W. Chen, J. Pan, T.A. Black, and A. Barr. 2003. Spatial distribution of carbon sources and sinks in Canada's forests based on remote sensing. *Tellus* **55B**: 622-641.
- Cramer W, A. Bondeau, F.I. Woodward, I.C. Prentice, R.A. Betts, V. Brovkin, P.M. Cox, V. Fisher, J. Foley, A.D. Friend, C. Kucharik, M.R. Lomas, N. Ramankutty, S. Sitch, B. Smith, A. White and C. Young-Molling. 2001 Global response of terrestrial ecosystem structure and function to CO₂ and climate change: results from six dynamic global vegetation models. *Global Change Biology* **7(4)**: 357-373.
- El Maayar, M., D.T. Price, C. Delire, J.A. Foley, T.A. Black and P. Bessemoulin. 2001. Validation of the Integrated Biosphere Simulator (IBIS) over Canadian deciduous and coniferous boreal forest stands. *J. Geophysical Research* **106**: 14,339-14,345.
- Foley, J.A., I.C. Prentice, N. Ramankutty, S. Levis, D. Pollard, S. Sitch, A. Haxeltine 1996. An integrated biosphere model of land surface processes, terrestrial carbon balance, and vegetation dynamics. *Global Biogeochemical Cycles*, **10(4)**: 603-623.
- Hughes, L. 2000. Biological consequences of global warming: is the signal already apparent? *Trends in Ecology and Evolution* **15**: 56-61.
- Hutchinson, M.F. 1998. Interpolation of rainfall data with thin plate smoothing splines: II analysis of topographic dependence. *J Geog. Information and Decision Analysis* **2(2)**: 168-185. http://publish.uwo.ca/~jmalczew/gida_4.htm

- Hutchinson, M.F. 2000. ANUSPLIN Version 4.0. <http://cres.anu.edu.au/outputs/anusplin.php>
- Hutchinson, M.F., and P.E. Gessler. 1994. Splines—more than just a smooth interpolator. *Geoderma* **62**: 45–67.
- IPCC (Intergovernmental Panel on Climate Change) 2001. Climate Change 2001: Working Group 1: The Scientific Basis. Summary for Policymakers. http://www.grida.no/climate/ipcc_tar/wg1/005.htm
- Kittel, T.G.F., J.A. Royle, C. Daly, N.A. Rosenbloom, W.P. Gibson, H.H. Fisher, D.S. Schimel, L.M. Berliner, and VEMAP2 Participants. 1997. A gridded historical (1895-1993) bioclimate dataset for the conterminous United States. In: Proc. 10th Conf. Applied Climatology, 20-24 October 1997, Reno, NV. American Meteorological Society, Boston, pp. 219–222.
- Kucharik, C.J.; J.A. Foley, C. Delire, V.A. Fisher, M.T. Coe, S.T. Gower, J.D. Lenters, C. Young-Molling, J.M. Norman and N. Ramankutty. 2000. Testing the performance of a dynamic global ecosystem model: Water balance, carbon balance, and vegetation structure. *Global Biogeochemical Cycles* **14(3)**: 795-825.
- Kurz, W.A. and M.J. Apps. 1999. A 70-year retrospective analysis of carbon fluxes in the Canadian Forest Sector. *Ecological Applications* **9(2)**: 526-547.
- Lacelle, B., C. Tarnocai, S. Waltman, J. Kimble, F. Orozco-Chavez and B. Jakobsen. 1997. North American Soil Carbon Map, Agriculture and Agri-food Canada, USDA, INEGI, Inst. of Geography, Univ. of Copenhagen.
- Lenihan, J.M. and R.P. Neilson. 1995. Canadian vegetation sensitivity to projected climatic change at three organizational levels. *Climatic Change* **30**: 27-56.
- McCarty, J. 2001. Ecological consequences of recent climate change. *Conservation Biology* **15**: 320-331.
- McKenney, D. W., M.F. Hutchinson, P. Papadopol, and D.T. Price. 2004. Evaluation of alternative spatial models of vapour pressure in Canada. Proc. Amer. Meteor. Soc. 26th Conference on Agricultural and Forest Meteorology, Vancouver, B.C., 23-26 August, 2004, 11 pp. CD-ROM.
- McKenney, D.W., J.H. Pedlar, P. Papadopol and M.F. Hutchinson. 2006a. The development of 1901–2000 historical monthly climate models for Canada and the United States. *Agric. For. Meteorol. in press*.
- McKenney, D., D. Price, P. Papadopol, M. Siltanen and K. Lawrence. 2006b. High-resolution climate change scenarios for North America. Frontline Technical Note No. 107, Can. For. Serv. Great Lakes Forestry Centre, Sault Ste. Marie. 6 pp.
- Mitchell, T.D., T.R. Carter, P.D. Jones, M. Hulme, and M. New. 2003: A comprehensive set of high-resolution grids of monthly climate for Europe and the globe: the observed record (1901-2000) and 16 scenarios (2001-2100). *J. Climate* submitted (but not published???) http://www.cru.uea.ac.uk/~timm/grid/CRU_TS_2_0.html
- Myneni, R. B., J. Dong, C. J. Tucker, R. K. Kaufmann, P. E. Kauppi, J. Liski, L. Zhou, V. Alexeyev and M. K. Hughes. 2001. A large carbon sink in the woody biomass of northern forests. *PNAS* **98(26)**: 14784-14789.
- Neilson, R. 1998. Simulated changes in vegetation distribution under global warming. In: The regional impacts of climate change: An assessment of vulnerability (Watson, R., Zinyowera, M. and Moss, R., editors), A Special Report of IPCC Working Group 2, Cambridge University Press, Cambridge, UK, pp. 441-456.
- Neilson, R.P. and VINCERA Researchers. 2006. Potential Catastrophic Dieback of North American Forests: What is the Price of Uncertainty? *Manuscript in preparation*.
- Norby, R.J., E.H. DeLucia, B. Gielen, C. Calfapietra, C.P. Giardina, J.S. King, J. Ledford, H.R. McCarthy, D.J.P. Moore, R. Ceulemans, P. De Angelis, A.C. Finzi, D.F. Karnosky, M.E. Kubiske, M. Lukac, K.S. Pregitzer, G.E. Scarascia-Mugnozza, W.H. Schlesinger, and R.

- Oren. 2005. Forest response to elevated CO₂ is conserved across a broad range of productivity. *PNAS* **162 (50)**: 18052-18056.
- Overpeck, J.T., P.J. Bartlein and T. Webb III. 1991. Potential magnitude of future vegetation change in Eastern North America: Comparisons with the Past. *Science*, **254**: 692-695.
- Parmesan, C. and G. Yohe. 2003. A globally coherent fingerprint of climate change impacts across natural systems. *Nature* **421**: 37-42.
- Penner, M., K. Power, C. Muirhead, R. Tellier, and Y. Wage. 1997. *Canada's Forest Biomass Resources: Deriving Estimates from Canada's Forest Inventory*, Pacific Forestry Centre, Canadian Forest Service, Victoria, Information Report No. BC-X-370.
- Price, D.T., D.W. McKenney, D. Caya, M.D. Flannigan and H.Côté. 2001. Transient climate change scenarios for high resolution assessment of impacts on Canada's forest ecosystems. Final report to Climate Change Action Fund, June 2001. http://www.cics.uvic.ca/scenarios/index.cgi?Other_Data#transienthighres
- Price, D.T., D.W. McKenney, I.A. Nalder, M.F. Hutchinson and J.L. Kesteven. 2000. A comparison of statistical and thin-plate spline methods for spatial interpolation of Canadian monthly mean climate data. *Agric. For. Meteorol.* **101**: 81-94.
- Price, D.T., D.W. McKenney, P. Papadopol, T. Logan, and M.F. Hutchinson. 2004. High resolution future scenario climate data for North America. Proc. Amer. Meteor. Soc. 26th Conference on Agricultural and Forest Meteorology, Vancouver, B.C., 23-26 August, 2004, 13 pp. CD-ROM.
- Rizzo, B. and E. Wiken. 1992, Assessing the sensitivity of Canada's ecosystems to climatic change. *Climatic Change* **21**: 37-55.
- Root, T., J. Price, K. Hall, S. Schneider, C. Rosenzweig and J.A. Pounds. 2003. Fingerprints of global warming on wild animals and plants. *Nature* **421**: 57-60.
- Scott, D. and C. Lemieux., 2005. Climate change and protected areas planning in Canada. *Forestry Chronicle*, Sept/Oct. 696-703.
- Scott, D., J. Malcolm and C. Lemieux. 2002. Climate Change and Biome Representation in Canada's National Parks System: Implications for System Planning and Park Mandates. *Global Ecology and Biogeography*, **11**: 475-484.
- Suffling, R. and D. Scott. 2002. Assessment of climate change effects on Canada's national park system. *Environmental Monitoring and Assessment* **74**: 117-139.
- VEMAP Members. 1995. Vegetation/ecosystems modelling and analysis project: Comparing biogeography and biogeochemistry models in a continental-scale study of terrestrial ecosystem responses to climate change and CO₂ doubling, *Global Biogeochemical Cycles* **9(4)**: 407-437.
- Woodward, F. and D. Beerling. 1997. The dynamics of vegetation change: health warnings for equilibrium 'dodo' models. *Global Ecology and Biogeography Letters* **6**: 413-418.

APPENDIX I

Summary of recent changes to IBIS – “Tower Flux Version”

David T. Price

Natural Resources Canada, Canadian Forest Service, Northern Forestry Centre,
5320-122 Street, Edmonton, Alberta. Canada T6H 3S5
dprice@nrcan.gc.ca

There are numerous changes to several modules. These have resulted from my attempts to resolve what I perceive to be serious problems in the calculation of hourly energy balances and various hypotheses about why these occur. One particular hypothesis was that canopy GPP was being seriously underestimated, which appears to be related to a poor representation of PAR absorption by the canopy – subroutines in RADIATION.F, notably TWOSTR(). I thought that the average canopy extinction was too high, resulting in light levels that are too low to allow positive photosynthesis in the lower canopy, or upper canopies with high LAI. Because each canopy is represented as a single leaf (or with sunlit/shaded algorithm, as two leaves), it is not possible to determine whether portions of the modelled canopy are operating below the light compensation point. If this was occurring in reality, the leaves would fall off, but in IBIS, the LAI is determined more empirically, so high LAI (or high cbiol()), is just a bigger respiration tax on canopy GPP. I thought this effect would lead to underestimates of NPP, and hence lower stomatal and canopy conductances, feeding back on transpiration and the energy balance.

Whether my hypothesis was right or wrong, it at least provided the basis for investigating causes of poor hourly energy balance. [It should be noted that I was not the only person concerned about this. Robert Grant looked at our output in early 2004 and thought that the energy balance results were very poor in comparison to other FLUXNET models. I agree with Mustapha that in general, we do get reasonable energy balances on a monthly or annual basis, but things fall apart at daily and hourly timescales.]

In late 2003 and early 2004, Fred Woslyng worked on several aspects, including:

3. Cleaning up and implementing a simplified version of Jinxun Liu’s N model code. There were numerous discrepancies between the final version Jinxun gave us, and what he described in his manuscript. Many of these differences were resolved in discussion with Jinxun. We set his soil decomposition “priming factor” (capafac) to 1.0 permanently. As far as I can tell it is not useful to change it to anything else. Fred also uncovered an “accounting error”, in STATS.F, SUMDAY(), in the summation of the calculated daily NPP, which basically meant that night time respiration was not being subtracted at leaf-level.
4. Jinxun’s code also supports a simple representation of dynamic allocation of C and N to plant biomass pools. I wanted Fred to investigate use of Vivek Arora’s dynamic C allocation that he is using in his CTEM model. We looked at the equations, but Fred did not have time to work on this. However, Jinxun’s code is running in DYNAVEG(). [I think this includes N feedbacks on conversion of NSC to structural biomass pools: Jinxun’s idea of “biomass construction efficiency”, which may mean that biomass accumulation is taxed, in addition to the respiration taxes taken off in SUMNOW()
5. Implementation and testing of Mustapha’s version of White & Running’s North American phenology code.

6. Developing the code needed to read in multiple soil types for a single gridcell, as available from the continental scale NAGSOIL data set. This required some significant modifications so that the land surface mask (file SURTA.NC) is expanded for every gridcell that contains two or more dominant soil types. In addition, the area fractions of each of these soil types must be carried into the calculations of gridcell totals and averages so that correct values are returned to the output files.
7. Many of the above modifications also required fixes to the handling of “restarts”, because additional state variables needed to be saved and restored when continuing a run with initial conditions generated by a previous run. This approach allows us to perform multiple comparison simulations for different GCM scenarios without rerunning the 1601-2000 spinup each time.

During summer of 2004, I picked away at the canopy light absorption issue (following discussions with the Madison group). I am not sure I achieved very much, but I did implement some simple constraints on the calculation of absorbed PAR for the upper and lower canopies. Both Marcus Costa and I (and I think Navin Ramankutty) observed that at low sun angles TWOSTR() can return h and k coefficients in termu() and terml() which result in impossible topparu() and topparl(). I.e., topparl() can be greater than topparu() (even though total incoming PAR at this point may be close to zero, so upper canopy should be absorbing all of it), and/or the total of topparu() and topparl() could exceed total incoming PAR. I added a simple trap to prevent this from happening: In such circumstances, 80% of total incoming PAR (sum of solad(i, 1) and solai(i, 1) is allocated to topparu() and topparl() in proportion to canopy LAIs.

Mustapha developed his sunlit/shaded algorithm, which I received in August or September 2004. Since then, my work on the TowerFlux version proceeded roughly as follows:

2. Implementation of Mustapha’s sunlit/shaded canopy photosynthesis code into my version of PHYSIOLOGY.F. The algorithm is commented at the top of STOMATA(). It uses subroutines to call the same code for each of C3 and C4 canopies, and for each of the 5 PFT classes, depending on their presence/absence in the simulated canopy. I found that straight swapping of the old “BIGLEAF” and the new “SUNSHAD” versions of the code resulted in quite significant increases in GPP and NPP.
3. I also tested Fred’s implementation of Jinxun’s N code and found that it runs pretty well. That is, turning off the variable C/N and instead setting Vm to the input Vmax resulted in higher values of GPP. Turning on variable C/N therefore lowers GPP, but it seems to be stable. Jinxun had imposed a constraint on soil mineral N content during the soil C pool spin-up phase. I have found that it is possible to remove this with only minor effect. In fact it seems to increase GPP and NPP slightly. I guess that his constraint was holding the mineral N content down (to 1.5 gN m⁻²), whereas the model wants to push it up towards 2.0 gN m⁻². I don’t know whether it is maintaining a level dynamically or just hitting another limit factor.
4. At some point, I was tracking changes in soil moisture and found a bug (which I discussed with Christine Delire) in SOILCTL(). I had seen this before, and I was very pleased with myself that I had now figured this out. It turns out that this was only the start of an intimate relationship with SOIL.F.
5. Once I had these two items running smoothly I started looking at the energy balance again. It seemed a little better. At some point, Fred and I decided that we should drop the new PHYSIOLOGY.F into his version of the spatial model. Fred had been running on Linux while I had been developing on Solaris, so it was time to check that we got similar results on the other platforms. BIG PROBLEM. We immediately found discrepancies. Fred resolved most of his, but I could not get decent agreement between the two

- platforms. In particular for the Campbell River site, there was no agreement and the two versions diverged rapidly as the simulation period was increased. After some discussion around the table, Fred suggested that it could be caused by a DIV0 floating point error (FPE). Neither platform produces executables which actually crash by default when FPEs occur. Certainly the Sun f77 executable reported DIV0. Robert Grant suggested that we should be able to trap the FPE. We found out how to do this with Sun f77. (DUH! – never thought of doing this before, mainly because I had come to expect that the error flags being raised at the end of a run were nothing to worry about unless NaNs appeared.)
6. I set up the FPE trap for DIV0 and found the problem. A single half-hourly data point for windspeed in the Campbell River data set was set to 0.0 (values in previous and next half-hour were about 1.5 m s^{-1}). Problem solved, but this did not result in perfect agreement between the two platforms. I decided to explore other FPEs. Over a period of several days, I tracked down, in turn, overflows and invalids reported for each of the four Fluxnet tower sites. Resolving these helped to remove some of the differences. In fact at one point I thought I had them all nailed but closer examination, with runs over longer periods there was still significant divergence.

In early 2005, Fred and I worked on modifications to leaf area growth (coupled to Jinxun's daily NPP, and dynamic allocation, to roots, foliage and residual to wood); use of current day's PLAI as a contributor to canopy total LAI; classification of LAI into five (now six) plant growth habits, each of which imposes an area-weighted control on factors influencing V_{\max} (N content, temperature, water stress); changes to phenological development criteria; low temperature constraints on survival of "warm PFTs"; removal of climatic determination of PFT existence, EXIST now depends entirely on NPP and FU/FL, with low temperatures ("frost") constraining northern limits of temperate and tropical PFTs.

During 2005 both of us have invested lots of effort on tuning species parameters. The usual procedure is to perform a run, examine the output and consider why it is wrong or how it can be improved. In some cases, this leads to further development in the algorithms, typically either by Mustapha or myself. These are tested initially using the tower flux version of the code, usually at four different Fluxnet sites for which Mustapha compiled data. When this seems to be working OK, a series of runs of the full spatial version are carried out where only parameters are adjusted to try to optimize the new algorithms.

In the course of 2005 we carried out approximately 200 separate runs of IBIS applied to North America: approximately 10,000 grid points, typically for 100 years. Fred has made many refinements to the scripts which have greatly improved reliability and performance. Using the Linux cluster (20 CPUs) and several additional multi-CPU systems available in the building, the typical execution time is about 10 hours for a 100-year run.

During this period (2005 to early 2006) we have implemented the following:

1. Modifications to temperature response of V_{\max} , based on original formulation but now made PFT specific. This has definitely improved temperature discrimination of PFTs but the results have been counter-intuitive; e.g., one might expect boreal PFTs to have lower temperature optima than temperate PFTs in order to grow better at higher latitudes, but this turns out not to be the case. Evidently, even though northern growing seasons are shorter, they are more continental and therefore warmer on average than some "temperate region" summers, and may therefore benefit from higher temperature optima.
2. PFT-specific respiration parameters, based on data from Ryan et al. (1997, JGR BOREAS Special Issue). The representation of stem and root respiration was rejigged to

- be in recognizable units rather than magic number “roll-ups”. I investigated treating leaf respiration as factor separate from GPP so that deciduous PFTs don’t have to pay a respiration tax in winter when leaves are no longer alive, but conversely, evergreens can take advantage of favourable conditions during fall and winter, while paying respiration taxes. This too seems to have worked reasonably well.
3. Introduction of Moss/Lichen PFT (mainly to provide a “low temperature grass” type at high latitudes). Moss “roots” are considered only to occupy the top soil layer (typically 10 cm or less, and therefore are very sensitive to moisture stress. This eventually required some modifications to the calculations of evapotranspiration from the lower canopy (see below).
 4. Splitting the Temperate Evergreen Conifer PFT into Cool (“west coast”) and Warm (“south eastern USA”) types. This is intended to capture the factors that are believed to contribute to coniferous forest dominating on the Pacific west coast (mild winters, wet springs and falls allow conifers to grow year round, while deciduous species are at a disadvantage competing during the summer when water deficits are common (low rainfall, and generally freely draining coarse textured soils on steep slopes (e.g. Franklin and Waring 1979). Conversely, some temperate needleleaf evergreen species are clearly adapted to warmer summers with higher rainfall, typical of the eastern seaboard in the USA and the Canadian maritime Provinces, and are able to compete effectively though deciduous species are dominant in this region.
 5. Splitting of Boreal Evergreen Conifer PFT into Dry (“pines”) and Moist (“spruces”) types. This is something that may prove superfluous. I resisted the temptation to do this for a long time, because the spatial scales at which boreal conifers can be split into dry and wet sites are much finer than the 10 to 50 km scale at which IBIS is being applied. Moreover, it is not entirely clear that such a discrimination is correct, though intuitively it seems so. However, the NAGSOIL data set clearly identifies large regions, including the Hudson Bay region, northern Saskatchewan and Alberta, and the border region extending from western NWT and eastern Alaska where organic soils are dominant. These soils are obviously “wet” soils: frequently saturated and cold, at least under current climate conditions. Before NAGSOIL, the soil textures were homogenized and less realistic. But now we are having difficulties getting boreal PFTs to grow successfully, and in some simulations (with parameters tuned) they have been completely devoid of significant leaf area. There could be several reasons, including short growing seasons and/or water stress (both caused by large ice contents in deep profiles), and N deficiencies caused by simulated N-immobilization in Jinxun Liu’s N model (though this does not appear to be causing soil N to disappear). In any case, creating a separate PFT that can survive under these conditions seems to be a good idea. It should have a lower optimal temperature range for V_{max} , have low tolerance for drought stress, and conversely, favour saturated conditions.
 6. Mustapha has developed and implemented improvements to representation of soil water stress effects on plant water uptake and its distribution in the soil profile, following Ph.D. work of Kaiyuan Li. (Paper in prep.). After some testing we are convinced that this is a significant advance, because it allows higher transpiration rates during periods of low soil water availability (and greater drawdown of soil water), as evidenced by comparisons at “dry” sites (Douglas-fir on Vancouver Island, and grassland sites in Alberta and California).
 7. Changes to multilayer soil texture profile so that: coarse freely draining mineral soils do indeed drain down while wet soils with impeded drainage stay wet. Rules to determine nature of bottom layer: mineral has sand at bottom, with relatively large BPERM (so that water drains and stays out of profile), while organic has clay at bottom with small BPERM (so that water stays in profile and only runs off when bucket is full). Played with

- idea of varying BPERM as a sine function of average slope, using slope data obtained from DEM data sets at higher resolution than the operational gridcells, but this does not appear to contribute much, probably because regions with steep slopes tend to have shallow coarse textured soils in any case.
8. Modifications to clay soil water holding capacity (“dynamic soil hydraulic conductivity”) to represent clay-cracking as a cause of increased infiltration when dry. This problem with clay soils turns out to be well-known in IBIS, but was not documented until recently. Communications with Christine Delire have helped to understand this, and we may try an alternative approach based on the Green and Ampt model of soil water movement.
 9. Implementation of water balance mass conservation checks and fixes to calculation of water stress so that reductions in profile water content match losses calculated for transpiration. This proved necessary to resolve an error in the allocation of water being transpired by the moss PFT, requiring a code modification to ensure moss LAI was coupled only to roots in the top soil layer, but contributed to total lower canopy LAI on equal terms.
 10. Representation of differential PFT responses to water stress (“dry”, “medium” and “wet”) with parabolic function to represent response to moisture content between saturation and wilting point (WP), also recognizing capacity of some plant types to extract water down to -2.5 MPa rather than more conventional definition of WP as -1.5 MPa.

APPENDIX II

CFS-NoFC North American Generalized Soil Data Set (NAGSOIL), Version 0.2.

Martin Siltanen and Travis Logan

Natural Resources Canada, Canadian Forest Service, Northern Forestry Centre,

5320-122 Street, Edmonton, Alberta. Canada T6H 3S5

(780)-435-7378

msiltane@nrcan.gc.ca

The CFS-NoFC North American Generalized Soil Data Set (NAGSOIL) 0.5 degree cell size soil data set is a series of map grids created using existing soil data bases from Alaska, Canada, and the United States.

For each grid cell representing the North American land mass, there may be up to four (4) mineral soil components, one (1) organic soil component, and one (1) non-soil component described.

The mineral and organic soil components are described using dominant and weighted-average conditions in three (3) vertical soil sections within that component. The soil sections are from 0-50, 50-100, and 100-150 cm depth.

The data set is organized into ASCII grids, one for each soil component (SOILNO), variable, and vertical soil section combination.

Gridded variables for each soil component are:

- component area within the 0.5 degree cell (km²),
- total soil depth (cm), and
- total organic thickness (cm).

Gridded variables for each mineral/organic soil component and soil section combination are:

- percent sand,
- percent clay,
- bulk density (g cm⁻³), and
- percent coarse fragments by volume.

Each grid represents the same land mass and extent. The ASCII grids may be imported into a GIS, converted to NetCDF format, or accessed directly as text files, depending on the user's requirements.

This document has two main sections:

- A) User Information – a short description of information needed by the user to access and understand the organisation of the grid files and data, and
- B) Development Information – a detailed description of the data set origins and the development of the data set.

TL-May 18, 2004 -initial data base write-up.
 MS-May 28, 2004 –initial spatial write-up
 MS-June 1, 2004 –version 0.1 draft README. V0.1 ASCII data set compiled.
 MS-July 23, 2004 –version 0.1 NetCDF data file and NetCDF README created.
 MS-Oct 22, 2004 -version 0.2 draft README: updated terminology and corrections.
 V0.2 ASCII data set compiled: corrections to VEMAP section3 (s, cl, bd, cf), Canada section3 at 100cm (s, cl, bd, cf), and –98 vs. 0 (s, cl, bd, cf).

A) USER INFORMATION

The GIS parameters of the ASCII grids are:

Number of rows:	120	Number of columns:	232
Coordinate system:	Geographic WGS 1984	Datum:	WGS 1984
Cell size:	0.5 degrees		
Extent:	Left –168, Right –52, Top 85, Bottom 25		

The ASCII grid file names describe the data in the grid. The name contains the soil number, variable name and, if applicable, vertical soil section number: e.g. grid name "s1_sa1.asg" is SOILNO 1, variable is percent sand, vertical soil section 1 (0-50cm). See Tables 1, 2, and 3 for coding explanations.

Table 1. Definition of soil component numbers (SOILNO) used in the data set.

SOILNO	Description
s1	-the most common mineral soil component by area within a cell, if present ¹ . -surface organic material is < 60 cm thick.
s2	-the 2 nd most common mineral soil component by area within a cell, if present. -surface organic material is < 60 cm thick.
s3	-the 3 rd most common mineral soil component by area within a cell, if present. -surface organic material is < 60 cm thick.
s4	-the least common mineral soil component by area within a cell, if present. -surface organic material is < 60 cm thick.
s5	-the organic soil component in the cell, if present. -the surface organic material is >= 60 cm thick.
s6	-the non-soil component in the cell, if present. -does not have any variable attributes other than area occupied.

¹ Cells may be represented by either mineral, organic, or non-soil components, individually or in any combination.

Table 2. Variables, their filename short forms, and descriptive information.

Variable	Short form	Data type	Description
area (km ²)	area	Integer	-area within the cell of the specified SOILNO. -the total of all SOILNO areas = total land area in the cell.
sand (%)	sa	Integer; range 0-100	-percent sand content by weight of the mineral soil < 2 mm. -may appear in 3 depth sections (0-50, 50-100, 100-150 cm).
clay (%)	cl	Integer; range 0-100	-percent clay content by weight of the mineral soil < 2 mm. -may appear in 3 depth sections (0-50, 50-100, 100-150 cm).
bulk density (g cm ⁻³)	bd	Float; range 0.00-2.00	-bulk density of the soil material < 2 mm. -may appear in 3 depth sections (0-50, 50-100, 100-150 cm).

coarse fragments (%)	cf	Integer; range 0-75	-coarse fragment (>2mm) content of the soil material. -may appear in 3 depth sections (0-50, 50-100, 100-150 cm).
total soil depth (cm)	td	Integer; max.392	-total depth of soil material; measured from the mineral surface in a mineral soil (excludes total organic thickness), or from the top of the organic surface in an organic soil (includes total organic thickness and any underlying mineral soil). -depth is limited by bedrock, permafrost, ice.
total organic thickness (cm)	to	Integer; max. 361	-total thickness of L, F, H, and/or O materials in the profile.

Table 3. Vertical soil sections, their filename short forms, and descriptive information.

Vertical soil section	Short form	Description
section 1	1	-vertical soil section from 0 – 50 cm ¹ .
section 2	2	-vertical soil section from >50 – 100 cm ¹ .
section 3	3	-vertical soil section from >100 – 150 cm ¹ .

¹ Soil section depth measured from top of the mineral soil, or from the top of the organic surface in an organic soil.

- Missing data value in a land cell is represented as "-98". The NODATA value for non-land cells is "-9999".
- There are discontinuities in the data due to the different data origins.
- The "na_id.asg" grid contains the unique, sequential, 0.5 degree cell identification number (NAID) for the land mass cells and can be used to trace the data back into the original data base files.
- Organic carbon data is not included due to reporting incompatibilities between the data sets.

B) DEVELOPMENT INFORMATION

The North American 0.5 degree soils data set was created in three steps:

- 1) organize and summarize all the data records for the soil components using a data base program,
- 2) generalize the spatial representation of the soil component distributions to a 0.5 degree cell size grid, and
- 3) combine the soil data records with the GIS grid cells to produce grids of soil variable information.

A point-form description of the general processing steps follows.

1) Organize and summarize the data records:

Data base records were taken from the Canadian Soil Information System (CanSIS) Soil Landscapes of Canada (SLC), the USDA State Soil Geographic (STATSGO) Database (for Alaska only), and the United States VEMAP Phase 1 publicly available soil data bases.

Data Sources:

- 1) US data (excluding Alaska) - Source: VEMAP Phase 1 database CD
http://www.cgd.ucar.edu/vemap/users_guide.html

- 2) Canadian data – CANSIS - SLC (soil landscapes of Canada) soil data set
<http://sis.agr.gc.ca/cansis/nsdb/slc/intro.html>
- 3) Alaska data - Source: USDA STATSGO digital soil dataset
<http://www.nrcs.usda.gov/products/datasets/statsgo/>

The data were manipulated into a common soils database format. The SLC and STATSGO data bases were in a similar GIS polygon and data base format. The VEMAP data were in 0.5 degree cell gridded format and were converted into a similar data base format as the SLC and STATSGO data.

The SLC and STATSGO soil component data sets consisted of soil layers of varying depths, texture, etc. The VEMAP data provided fixed soil layer depths. (See the respective data set manuals for a complete description of data organization.)

For SLC and STATSGO, the soil data were summarized using a database program into three depth sections (0-50, 50-100, 100-150 cm) for each soil component within a polygon spatial unit. For VEMAP, the data were provided in two depth sections, 0-50 and 50-150 cm, which were divided into three depth sections (0-50, 50-100, 100-150 cm) as soil depth warranted.

All soil components were tagged as being either mineral or organic soil based on:

- Canada and Alaska datasets: Organic soil defined as a soil profile with 60cm or more of organic material (based on the Canadian Soil Classification System).
- USA dataset: The VEMAP data set identified areas within each cell as being organic, if present.

Soil depth measurement criteria:

- Mineral Soils - all depth measurements are made from the upper surface of the top-most mineral horizon in the profile.
- Organic Soils - all depth measurements are made from the top organic surface of the profile (excluding litter).
- Canada data – total depth of organic soil is determined by the total thickness of SLC – Layer 1 (which is defined as containing L, F, H, and/or O), and Layer 2 if it is designated O.
- Alaska data – total thickness of organic soil is determined by the addition of soil layers with STATSGO soil texture classes of:
 - Fibric Material
 - Hemic Material
 - Mucky-Peat
 - Muck
 - Peat
- USA data - VEMAP data contains a depth variable for each mode.

Reported soil depths are the depth of soil components down to a declared bottom depth in the originating data set or the start of non-soil layers. Non-soil layers consist of material such as bedrock, scree, unconsolidated rock, and permafrost/ice.

Soil layer texture classes present in the SLC and STATSGO data bases were assigned %sand and % clay values representing the modal condition of the soil texture classes (Table 4) (taken from the standard soil texture triangle). VEMAP provided %sand and % clay data for each section.

Table 4. Modal soil texture values (% sand, silt, clay) assigned to soil texture classes in the Canadian and Alaskan data sets.

Soil texture class	Sand %	Silt %	Clay %
clay	27	22	51
clay loam	33	34	33
heavy clay*	13	13	74
loam	41	40	19
loamy sand	81	13	6
sand	92	5	3
sandy clay	51	7	42
sandy clay loam	60	13	27
sandy loam	64	25	11
silt	8	87	5
silt loam	22	65	13
silty clay	6	47	47
silty clay loam	10	56	34

*Canadian dataset only

Coarse fragment content for the SLC and STATSGO data sets were assigned based on the coarse fragment modifier of the soil texture class for that section, if present (Table 5). The VEMAP data set provided rock fragment (%) data for each section.

Table 5. Coarse Fragment (%) content values in SLC and STATSGO soil texture classes.

Soil texture modifier	Stones %	Cobbles %	Gravel %	Coarse fragments %
stony	25			25
cobbly		25		25
gravelly			25	25
very stony	50			50
very cobbly		50		50
very gravelly			50	50
extremely stony	75			75
extremely cobbly		75		75
extremely gravelly			75	75

Soil profile values within each soil component for SLC and STATSGO were standardized in the data base program as follows

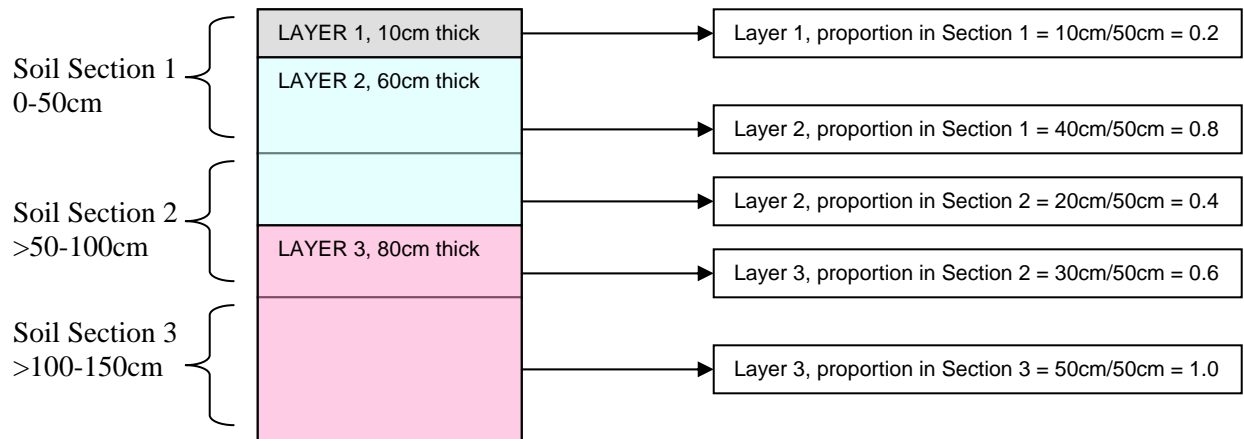
- Soil texture values, coarse fragment percentages, and bulk density values were summarized for each soil component using a thickness-weighted average of the

values from various soil layers that occur in three soil sections: 1) 0 - 50cm, 2) >50 - 100cm, and 3) >100 - 150cm.

Weighted averaging consisted of a multi-step process:

1. Determining the proportional weight based on the thickness of each reported soil layer in the SLC or STATSGO data set that occurs in each of the standard soil sections.
2. Multiplication of that proportion with its corresponding soil profile values (% sand, silt, clay, coarse fragments, bulk density) to get weighted values for each soil section.
3. Addition of the weighted values for each soil section to obtain the weighted average value for that soil section.

Figure 1. Example of thickness-weighted averaging procedure.



Therefore the standardized value of, for example, *%sand in soil section 1* equals:

$$0.2 * (\% \text{ sand value Layer1}) + 0.8 * (\% \text{ sand value Layer2})$$

and *%sand in soil section 2* equals:

$$0.4 * (\% \text{ sand value Layer2}) + 0.6 * (\% \text{ sand value layer3})$$

and *%sand in soil section 3* equals:

$$1.0 * (\% \text{ sand value layer3})$$

In cases of organic soil overlaying mineral at depth, unaveraged mineral soil texture values were carried through for the appropriate section (e.g. 100-150cm) if the mineral proportion in the section was greater than or equal to 50% of the section thickness. Otherwise, the section received the organic values. As such it is possible to have

locations of “Organic Soil” which still have texture values (sand, silt, clay) in sections 2 and/or 3.

In Canada the most common soil profile depth is 100cm due to the original SLC summary procedure generally limiting data to that depth. As such, if the profile reaches 100cm then it was assumed that in reality it likely continued deeper. Hence the deepest soil layer values were simply extended down into section 3 (100-150 cm) to the depth of 150 cm. However, if the profile is reported to be shallower than 100 cm depth the data were not extended down into section 3.

2) Generalize the spatial representation:

The SLC and STATSGO polygons contained a polygon identifier (PID) and one or more soil components as records within the same polygon each with a component identifier (CMPID). Each VEMAP 0.5 degree cell had eight soil "modes" (four mineral and four organic). These VEMAP modes were treated the same as the soil components for SLC and STATSGO, so each was given a CMPID (modes #'s 1 to 4 were mineral, 5 to 8 were organic).

Using the PID as a data value, the original SLC and STATSGO polygon coverages were converted using Arc/Info POLYGRID to a 1 km cell size grid (Lambert Azimuthal projection) and merged together. This helped to preserve relative area distribution of the polygons in the initial aggregation procedure. The 1 km grid was then aggregated to a 10 km cell size and classified with a single PID using simple area dominance within the 10 km grid cell (i.e. the PID that occupied the most 1 km cells was taken as the PID for the 10 km cell).

The 10 km Lambert conformal grid was projected to a 0.083 degree Geographic grid.

A 0.5 degree square cell grid was imposed on the entire North American land mass using a window extent that coincided with the VEMAP 0.5 degree grid. Each cell in this North American 0.5 degree grid was given a new North American cell identifier (NAID).

For the 0.5 degree grid area representing the SLC and STATSGO data bases, a 0.083 degree grid of the fractional area that each 0.083 cell occupied within it's corresponding NAID 0.5 degree grid cell was created. The summed fractions for each PID at 0.083 degree cell size within a 0.5 degree cell were used to calculate the corresponding PID percent within each 0.5 degree cell. VEMAP provides a percent land mass value of each "mode" for each 0.5 degree grid cell. This gives us a PID percent within each NAID cell for the entire NA 0.5 degree grid.

A "reference area" data file (REFAREA) was created that corresponds to the PID percent data. For SLC and STATSGO, the PID % relates to the 0.5 degree grid cell area; for VEMAP the PID % relates to the VEMAP land mass area within each 0.5 degree cell. This is used later to calculate the actual soil group areas in each 0.5 degree cell.

The listing of NAID's and corresponding PID's was used to subset the soil data records. Only the soil component data records for PID's having some area within a NAID 0.5 degree cell were retained in the soil record data base.

3) Combine the soil data records with the GIS grid cells

The REFAREA value was relationally joined to the data records. An actual area in km² of each soil component was calculated ($CMP_KM2 = PID\% * CMPID\% * REFAREA$).

Data records having the identical combination of NAID, %sand0-50, %sand50-100, %clay0-50, and %clay50-100 values were summarized into one record by sorting into descending area coverage and choosing the variable values from the record with the largest area. The area values were summed. This reduced the number of records per NAID dramatically.

The remaining mineral component records were sorted into descending area size by 0.5 degree cell and compared. It was discovered that, overall, the largest four components occupied > 98% of the total mineral soil area. To reduce the number of mineral soil components for each 0.5 degree cell, the four largest mineral soil components in each cell were retained as representative of the mineral soils in the cell. Their area coverages within each cell were scaled up proportionally to occupy the total mineral soil area in that cell.

There were fewer organic component records in total and per 0.5 degree cell. The organic records were summarized into one record per 0.5 degree cell calculating weighted averages of bulk density, total organic depth, and total depth for each organic component and then summing the results by cell. The other variable data for the summarized record were taken from the organic component with the largest area coverage because sand, clay, and coarse fragment values may become nonsensical if averaged.

The summarized mineral and organic records were given final soil component numbers (SOILNO). The SOILNO's are:

- 1 – mineral soil with largest area coverage
- 2 – mineral soil with 2nd largest area coverage
- 3 – mineral soil with 3rd largest area coverage
- 4 – mineral soil with 4th largest area coverage
- 5 – organic soil
- 6 – non-soil (land without soil attributes)

Not all cells will have valid data for each SOILNO. Some cells may have only non-soil or organic components.

Non-soil data were taken from the original SLC and STATSGO data sets if present. For the VEMAP data set the non-soil component was calculated from the given data by subtracting the total mineral/organic area from the total landmass area.

The final NA 0.5 degree soil component data file was joined to the base NAID GIS attribute table. Individual GIS grids were created from this master GIS grid and table and then exported to create ASCII grids of each variable. If no data were available for a specific variable, -98 was used as the missing data value. The non-land cells were assigned the value -9999.